
Complete Set of Solutions of the Generalized Bloch Equation

K. KOWALSKI, P. PIECUCH

Department of Chemistry, Michigan State University, East Lansing, MI 48824

Received 20 April 2000; revised 18 July 2000; accepted 27 July 2000

ABSTRACT: The genuine multireference approaches, including multireference coupled-cluster (MRCC) methods of the state-universal and valence-universal type, are based on the generalized Bloch equation. Unlike the Schrödinger equation, the Bloch equation is nonlinear and has multiple solutions. In this study, the homotopy method is used to obtain complete sets of solutions of the exact and approximate Bloch equations for a four-electron model system consisting of four hydrogen atoms. Different geometries of the model and different choices of the multidimensional reference space are investigated. The rigorous relationships between the solutions of the Bloch equation corresponding to approximate and exact cases are established by extending the procedure of β -nested equations to multireference case. It is argued that the nonlinear nature of the Bloch equation and the asymmetric treatment of the excitation manifolds corresponding to different reference configurations in the Bloch wave operator formalism are the primary reasons for the emergence of various problems plaguing genuine MRCC calculations, including the recently discovered intruder solution problem [K. Kowalski and P. Piecuch, *Phys. Rev. A* **61**, 052506 (2000)]. © 2000 John Wiley & Sons, Inc. *Int J Quantum Chem* **80**: 757–781, 2000

Key words: multireference approaches; the Bloch equation; intruder solution problem; nonlinear equations; homotopy method

1. Introduction

The Bloch equation and the wave operator formalism [1–3] provide a basis for the genuine multireference coupled-cluster (MRCC) theories that are designed to describe ground and excited quasidegenerate electronic states. Examples of the genuine MRCC theories are the state-universal (SU)

Correspondence to: P. Piecuch; e-mail: piecuch@cem.msu.edu.
Internet: www.cem.msu.edu/~piecuch.

CC [4–17] and valence-universal (VU) CC (see Refs. [17–20], and references therein) methods.

The most characteristic feature of the Bloch equation is its nonlinearity. The exponential nature of the CC ansatz [17, 21–24], used in the SUCC and VUCC methods, increases the nonlinearity of the resulting equations for cluster amplitudes even further. In consequence, in the SUCC and VUCC calculations one has to deal with a problem of multiple solutions of the equations for cluster operators [9, 14, 20]. In addition, the MRCC calculations are plagued

by intruder states. Intruder states cause problems with converging the desired physical solution of the MRCC equations and are blamed for the significant deterioration of the quality of the results, when the ground state becomes nondegenerate.

Normally, the existence of intruder states is related to divergent nature of the corresponding multireference many-body perturbation theory (MRMBPT) energy and wave function expansions [25–29]. However, as pointed out in Ref. [14], the MRCC equations represent systems of nonlinear algebraic equations, so that problems plaguing MRCC theories do not necessarily have to be the same as problems appearing in MRMBPT calculations. Because of the algebraic nature of all MRCC theories, there is a need for nonperturbative explanation of the origin of problems plaguing MRCC calculations. After all, despite the fact that much attention has been paid to the intruder state problem of the MRMBPT formalism, practically none of the existing genuine MRCC approaches can routinely be applied in calculations of ground- and excited-state potential energy surfaces. Therefore, there is a need for a better understanding of the fundamental nature of convergence and other problems plaguing genuine MRCC methods.

Our recent mathematical and numerical analysis of multiple solutions of the SUCC equations [14] indicates that there exist solutions of nonlinear SUCC equations, referred to as the *intruder solutions*, that are responsible for numerical problems with solving the SUCC equations in the nondegenerate regime. In order to learn to what extent the *intruder solution problem* discovered in Ref. [14] is caused by the Bloch equation itself, in this work we analyze complete sets of solutions of different variants of the Bloch equation. As in Ref. [14], multiple solutions of the Bloch equation are obtained with the homotopy method [24, 30–32]. We use the homotopy method to find all solutions of the Bloch equation for the four-electron molecular system, referred to as the P4 model [33]. In order to provide additional insight into the origin and interpretation of multiple solutions of the approximate and exact forms of the Bloch equation, we generalize the formalism of β -nested equations (β -NEs) [24, 34] to the multireference case. The multireference β -NE formalism and homotopy calculations allow us to demonstrate that the intruder solution problem is largely a consequence of the nonlinear character of the Bloch equation and the asymmetric treatment of the excitation manifolds corresponding to different reference configurations in approximate forms

of the Bloch equation. The particular form of the wave operator is of lesser importance.

Along with our earlier work [14], this study can be regarded as a step toward nonperturbative explanation of the origin of problems plaguing genuine MRCC theories. By solving the Bloch equation directly, we can also suggest new ways of solving the MRCC equations of the SUCC type. One such method is briefly discussed at the end of this work. Solving the Bloch equation directly may also lead to new types of genuine multireference approaches of non-CC type. The BCID method discussed in this study is an example of the configuration-interaction-like (CI-like) multireference approach resulting from solving the Bloch equation directly. Other types of methods based on the direct iterative algorithm for solving the Bloch equation have recently been examined by Meißner and Paldus [35] (cf., also, Ref. [36] for related work).

2. Wave Operator Formalism and the Bloch Equation

2.1. OPERATOR FORMULATION

In all genuine multireference theories, we assume that there exists a multidimensional *model* or *reference space* \mathcal{M}_0 ,

$$\mathcal{M}_0 = \text{ls}\{|\Phi_q\rangle\}_{q=1}^M, \quad (1)$$

spanned by a suitably chosen set of the configuration state functions $|\Phi_q\rangle$, which provides a reasonable zero-order description of the *target space* \mathcal{M} ,

$$\mathcal{M} = \text{ls}\{|\Psi_\mu\rangle\}_{\mu=1}^M, \quad (2)$$

spanned by a finite number of the exact wave functions $|\Psi_\mu\rangle$ satisfying the electronic Schrödinger equation,

$$H|\Psi_\mu\rangle = E_\mu|\Psi_\mu\rangle. \quad (3)$$

The wave operator U ,

$$U: \mathcal{M}_0 \rightarrow \mathcal{M}, \quad (4)$$

is defined as a one-to-one mapping between \mathcal{M}_0 and \mathcal{M} that satisfies the following relations:

$$PU = P, \quad (5)$$

$$UP = U, \quad UQ = 0, \quad (6)$$

where

$$P = \sum_{q=1}^M P_q = \sum_{q=1}^M |\Phi_q\rangle\langle\Phi_q| \quad (7)$$

is the projection operator onto the model space \mathcal{M}_0 and

$$Q = 1 - P = \sum_{j=M+1}^{N_C} |\Phi_j\rangle\langle\Phi_j| \quad (8)$$

is the projection operator onto the orthogonal complement of \mathcal{M}_0 , i.e., \mathcal{M}_0^\perp . Here and elsewhere in the present study, N_C designates the number of configuration state functions corresponding to the full CI (FCI) problem for those eigenstates $|\Psi_\mu\rangle$ that have a nonzero overlap with \mathcal{M}_0 , i.e., the dimension of the relevant N -electron Hilbert space \mathcal{H}_N . The indices p, q are used to label the configuration state functions that span \mathcal{M}_0 and indices j, k label the configurations that belong to \mathcal{M}_0^\perp . The Greek letters γ, δ are used to label all configuration state functions, independent of whether they belong to \mathcal{M}_0 or \mathcal{M}_0^\perp . Equation (5) represents the so-called *intermediate normalization condition* of the Bloch wave operator formalism. Based on Eqs. (5) and (6), one can show that $U^2 = U$, although, unlike P and Q , the wave operator U is not Hermitian, $U \neq U^\dagger$.

The wave operator U satisfies the energy-independent equation,

$$HU = UHU, \quad (9)$$

which is referred to as the generalized Bloch equation [1–3]. Once the wave operator is determined by solving Eq. (9), the energies E_μ , $\mu = 1, \dots, M$, are obtained by diagonalizing the *effective Hamiltonian*,

$$H^{\text{eff}} \equiv H^{\text{eff}}(U) = PHU = PHUP, \quad (10)$$

within the model space \mathcal{M}_0 . The corresponding wave functions $|\Psi_\mu\rangle$, $\mu = 1, \dots, M$, are obtained from the formula,

$$|\Psi_\mu\rangle = U \left(\sum_{q=1}^M c_{q,\mu} |\Phi_q\rangle \right) = \sum_{q=1}^M c_{q,\mu} U |\Phi_q\rangle, \quad (\mu = 1, \dots, M), \quad (11)$$

where vectors $\mathbf{c}_\mu = (c_{1,\mu}, \dots, c_{M,\mu})$, $\mu = 1, \dots, M$, are the right eigenvectors of the non-Hermitian matrix $\mathbf{H}^{\text{eff}}(U) \equiv \|\langle\Phi_p|H^{\text{eff}}(U)|\Phi_q\rangle\|_{p,q=1}^M$ representing the operator $H^{\text{eff}}(U)$, Eq. (10). It must be emphasized that different wave operators U obtained by solving Eq. (9) lead to different effective Hamiltoni-

ans $H^{\text{eff}}(U)$. Each solution of Eq. (9) leads to a particular set of M energies E_μ and wave functions $|\Psi_\mu\rangle$. Different sets of energies and wave functions (different target spaces \mathcal{M}) are obtained for different operators U satisfying Eq. (9).

In the language of many-body quantum mechanics, the wave operator U can uniquely be represented as follows:

$$U = \sum_{q=1}^M (1 + C^{(q)}) P_q, \quad (12)$$

where each excitation operator $C^{(q)}$ is a sum of its many-body components $C_i^{(q)}$ that, when acting on $|\Phi_q\rangle$, produce the excited configurations belonging to \mathcal{M}_0^\perp ,

$$C^{(q)} = \sum_{i=1}^N C_i^{(q)}, \quad (q = 1, \dots, M). \quad (13)$$

For each i -body component $C_i^{(q)}$, we can write

$$C_i^{(q)} = \sum_{I^{(i)}} {}^{(q)}f_{I^{(i)}} {}^{(q)}G_{I^{(i)}}, \quad (q = 1, \dots, M), \quad (14)$$

where ${}^{(q)}G_{I^{(i)}}$ are the usual excitation operators generating the i -tuply excited configurations relative to $|\Phi_q\rangle$ and ${}^{(q)}f_{I^{(i)}}$ are the corresponding CI-like expansion coefficients. The operators ${}^{(q)}G_{I^{(i)}}$ that describe excitations into the model space are not included in $C_i^{(q)}$, since U satisfies the intermediate normalization condition, Eq. (5).

The Bloch equation (9) is nonlinear in U . Thus, already in the simplest case of the CI-like parametrization of the wave operator U , implied by Eqs. (12)–(14), the Bloch equation is bilinear in $C_i^{(q)}$ or coefficients ${}^{(q)}f_{I^{(i)}}$ that describe $C_i^{(q)}$. The MRCC exponential parametrizations increase the nonlinearity of the Bloch equation even further. For example, in the SUCC theory, U is represented as follows [4]:

$$U = \sum_{q=1}^M e^{T^{(q)}} P_q, \quad (15)$$

where

$$T^{(q)} = \sum_{i=1}^N T_i^{(q)}, \quad T_i^{(q)} = \sum_{I^{(i)}} {}^{(q)}t_{I^{(i)}} {}^{(q)}G_{I^{(i)}} \quad (16)$$

are the SUCC cluster operators, with ${}^{(q)}t_{I^{(i)}}$, representing the relevant cluster amplitudes.

In the exact theory, in which all many-body components $C_i^{(q)}$ and $T_i^{(q)}$, $i = 1, \dots, N$, are included in $C^{(q)}$ and $T^{(q)}$, respectively, the linear parametrization of U , Eq. (12), and the nonlinear parametrization of U , Eq. (15), give identical results, i.e., both parametrizations lead to exact energies E_μ and exact wave functions $|\Psi_\mu\rangle$, $\mu = 1, \dots, M$. The differences between the CI-like parametrization of U , Eq. (12), and the exponential parametrizations of U , Eq. (15), arise when the many-body expansions of $C^{(q)}$ and $T^{(q)}$ are truncated.

Truncated SUCC and other genuine MRCC formalisms are plagued by several problems described in the Introduction. By solving the Bloch equation directly, we should be able to learn to what extent these problems are related to the nonlinear nature of Eq. (9).

2.2. MATRIX FORMULATION

In order to solve the Bloch equation directly, it is convenient to introduce the matrix representation of the wave operator U in the basis set composed of the reference configurations $|\Phi_q\rangle$, $q = 1, \dots, M$, and the \mathcal{M}_0^\perp configurations $|\Phi_k\rangle$, $k = M + 1, \dots, N_C$. From Eqs. (5) and (6), it immediately follows that the only matrix elements $U_{\gamma\delta} \equiv \langle \Phi_\gamma | U | \Phi_\delta \rangle$ that need to be considered are

$$U_{pq} = \langle \Phi_p | U | \Phi_q \rangle = \delta_{pq}, \tag{17}$$

$$U_{kq} = \langle \Phi_k | U | \Phi_q \rangle = \langle \Phi_k | C^{(q)} | \Phi_q \rangle, \tag{18}$$

where, according to our notation, $|\Phi_p\rangle, |\Phi_q\rangle \in \mathcal{M}_0$, $|\Phi_k\rangle \in \mathcal{M}_0^\perp$. In terms of these matrix elements, the wave operator U can be written as follows:

$$U = \sum_{p,q=1}^M |\Phi_p\rangle \delta_{pq} \langle \Phi_q| + \sum_{q=1}^M \sum_{k=M+1}^{N_C} |\Phi_k\rangle U_{kq} \langle \Phi_q|, \tag{19}$$

since

$$U = UP = (P + Q)UP = PUP + QUP = P + QUP. \tag{20}$$

Since $U_{pq} = \delta_{pq}$ [cf. Eq. (17)], the only matrix elements $U_{\gamma\delta}$ that need to be determined are matrix elements U_{kq} , $k = M + 1, \dots, N_C$, $q = 1, \dots, M$. In order to obtain equations for these matrix elements, we project the Bloch equation (9) from the left on $|\Phi_j\rangle$, $j = M + 1, \dots, N_C$, and from the right on $|\Phi_p\rangle$, $p = 1, \dots, M$. We obtain,

$$H_{jp} + \sum_{k=M+1}^{N_C} H_{jk} U_{kp} =$$

$$\sum_{q=1}^M \sum_{k=M+1}^{N_C} U_{jq} H_{qk} U_{kp} + \sum_{q=1}^M U_{jq} H_{qp}, \tag{21}$$

$(j = M + 1, \dots, N_C; p = 1, \dots, M),$

where $H_{\gamma\delta} = \langle \Phi_\gamma | H | \Phi_\delta \rangle$. Projection of Eq. (9) from the left on $|\Phi_q\rangle$ would only result in a trivial identity equivalent to the equation $PHU = PUHU$.

Clearly, Eq. (21) represents a system of bilinear polynomial equations for the $(N_C - M) \times M$ unknown matrix elements U_{kq} . Once this system is solved, we construct the matrix of the effective Hamiltonian, $\mathbf{H}^{\text{eff}}(U)$, using the formula,

$$H_{pq}^{\text{eff}}(U) = \langle \Phi_p | HU | \Phi_q \rangle = H_{pq} + \sum_{k=M+1}^{N_C} H_{pk} U_{kq}, \tag{22}$$

$(p, q = 1, \dots, M).$

Diagonalization of $\mathbf{H}^{\text{eff}}(U)$ gives the final energies E_μ and the corresponding eigenvectors \mathbf{c}_μ , $\mu = 1, \dots, M$, which can be used to obtain the final wave functions $|\Psi_\mu\rangle$ [cf. Eq. (11)]. It is worth noticing that matrix elements of the effective Hamiltonian, $H_{pq}^{\text{eff}}(U)$, allow us to rewrite Eq. (21) in a quasi-linearized form,

$$H_{jp} + \sum_{k=M+1}^{N_C} H_{jk} U_{kp} = \sum_{q=1}^M U_{jq} H_{qp}^{\text{eff}}(U), \tag{23}$$

$(j = M + 1, \dots, N_C; p = 1, \dots, M),$

which can be very convenient for developing the iterative methods of solving the Bloch equation. Clearly, the system of Eqs. (22) and (23) is equivalent to Eq. (21).

Symbolically, the system of nonlinear equations (21) can be given the following form:

$$\mathbf{F}(\mathbf{x}) = \mathbf{0}, \tag{24}$$

where \mathbf{x} designates the vector of the unknown matrix elements of the wave operator U , $\mathbf{x} = (\dots, U_{jp}, \dots)$, and $\mathbf{F}(\mathbf{x}) = (\dots, F_{jp}(\mathbf{x}), \dots)$, with the individual components $F_{jp}(\mathbf{x})$ defined as

$$F_{jp}(\mathbf{x}) = H_{jp} + \sum_{k=M+1}^{N_C} H_{jk} U_{kp} - \sum_{q=1}^M U_{jq} H_{qp} - \sum_{q=1}^M \sum_{k=M+1}^{N_C} U_{jq} H_{qk} U_{kp}, \tag{25}$$

$(j = M + 1, \dots, N_C; p = 1, \dots, M).$

It should be noticed that the components of the vector function $\mathbf{F}(\mathbf{x})$ and the components of \mathbf{x} are labeled by two indices, j and p , that correspond to configurations from \mathcal{M}_0^\perp and \mathcal{M}_0 , respectively.

Thus, Eq. (25) is a system of $(N_C - M) \times M$ bilinear equations for the $(N_C - M) \times M$ unknowns U_{jp} . Approximate forms of the matrix Bloch equation, Eqs. (24) and (25) or (21)–(23), can be obtained by restricting the values of j and k in Eq. (25) to values corresponding to those \mathcal{M}_0^\perp configurations $|\Phi_j\rangle$ that are included in the calculations. The BCID approximation introduced in the next section is obtained by simply limiting the \mathcal{M}_0^\perp configurations $|\Phi_j\rangle$ to biexcited configurations relative to each of the M references $|\Phi_p\rangle$.

Our recent study of multiple solutions of the SUCCD (SUCC with doubles) equations [14] demonstrates that the truncated SUCC equations have the so-called *intruder solutions*, which may cause serious numerical problems in obtaining the physical solution in the nondegenerate regime. Each of these intruder solutions is characterized by the small overlap of the corresponding target space \mathcal{M} with the model space \mathcal{M}_0 in the quasidegenerate region and large overlap with \mathcal{M}_0 in other regions. As demonstrated in Ref. [14], in the quasidegenerate region, in which M eigenstates $|\Psi_\mu\rangle$ of the electronic Hamiltonian are clearly separated from the rest of the electronic spectrum, the overlap of the target space \mathcal{M} corresponding to the intruder solution of truncated SUCC equations with the target space representing the physical solution (M quasidegenerate states $|\Psi_\mu\rangle$) is small. This is why no problems arise with obtaining and identifying the physical solution of truncated SUCC equations in the quasidegenerate region. However, in all other (i.e., nondegenerate) regions, in which a given set of M eigenstates $|\Psi_\mu\rangle$ is no longer clearly separated from the rest of the electronic spectrum, the wave functions corresponding to intruder solutions gain significant \mathcal{M}_0 components and the overlaps of target spaces \mathcal{M} corresponding to intruder solutions with the target space representing the physical solution become relatively large. In consequence, obtaining a physical solution of truncated SUCC equations in the nondegenerate region with standard numerical algorithms becomes a major problem. In fact, in the nondegenerate region, the energies and wave functions provided by intruder solutions may be better than the energies and wave functions provided by the physical solution [14].

As pointed out in Ref. [14], and as implied by theorems discussed in Ref. [14], there are two reasons for the emergence of the *intruder solution problem* in truncated SUCC calculations: the nonlinear parametrization of the wave operator used in the SUCC theory and the Bloch equation itself. In order to

learn to what extent the intruder solution problem is associated with the particular parametrization of the wave operator, we use the homotopy method to obtain a *complete set of solutions* of the matrix Bloch equation, Eqs. (24) and (25). Both the exact and approximate forms of the matrix Bloch equation are investigated.

3. Homotopy Method

In the homotopy method [30–32], in order to find all geometrically isolated solutions of a system of polynomial equations (24) [in our case, the individual components of $\mathbf{F}(\mathbf{x})$ have a particular form of Eq. (25)], we consider a family of equations,

$$\mathbf{H}(\mathbf{x}, \lambda) = (1 - \lambda)\mathbf{G}(\mathbf{x}) + \lambda\mathbf{F}(\mathbf{x}) = \mathbf{0}, \quad (26)$$

where $\mathbf{G}(\mathbf{x})$ is chosen in such a way that all solutions of a system of equations $\mathbf{G}(\mathbf{x}) = \mathbf{0}$ are known and λ is the continuation parameter ($\lambda \in [0, 1]$). For $\lambda = 0$, Eq. (26) reduces to $\mathbf{H}(\mathbf{x}, 0) = \mathbf{G}(\mathbf{x}) = \mathbf{0}$, whereas for $\lambda = 1$, we obtain $\mathbf{H}(\mathbf{x}, 1) = \mathbf{F}(\mathbf{x}) = \mathbf{0}$. If each component of the vector function $\mathbf{G}(\mathbf{x})$ is defined as $G_\alpha(\mathbf{x}) = x_\alpha^{d_\alpha} - \rho_\alpha$, where $d_\alpha \geq \deg F_\alpha$ [$\deg F_\alpha$ designates the total degree of the polynomial F_α , where F_α is the α component of $\mathbf{F}(\mathbf{x})$], and if the parameters ρ_α are chosen randomly, then the Transversality Theorem [30, 31] guarantees that all solutions of the system of equations $\mathbf{F}(\mathbf{x}) = \mathbf{H}(\mathbf{x}, 1) = \mathbf{0}$ can be obtained by continuation of all solutions of $\mathbf{G}(\mathbf{x}) = \mathbf{H}(\mathbf{x}, 0) = \mathbf{0}$. Since the matrix form of the Bloch equation, Eqs. (24) and (25), is bilinear in U_{jp} , we used the following definition of $G_\alpha(\mathbf{x})$:

$$G_\alpha(\mathbf{x}) \equiv G_{jp}(\mathbf{x}) = U_{jp}^2 - \rho_{jp} \equiv x_\alpha^2 - \rho_\alpha, \quad \alpha = (jp), \quad (27)$$

where $p = 1, \dots, M$, and for each p , index j labels the \mathcal{M}_0^\perp configurations included in calculations (in the exact theory, $j = M + 1, \dots, N_C$; in approximate theories, the range of j values for each reference configuration $|\Phi_p\rangle$ can be different). For solving the matrix Bloch equation, Eqs. (24) and (25), with the homotopy method, we used HOMPACK [32].

4. Computational Details and Model Description

In order to obtain the complete set of solutions of the Bloch equation, we have carried out a series of the homotopy calculations for the minimum basis set P4 model consisting of four hydrogen atoms

in rectangular arrangement and described by four $1s$ -type atomic orbitals centered on the hydrogen nuclei [33]. The geometry of the P4 model is determined by a single parameter α , which is defined as a distance between two slightly stretched H_2 molecules (the H–H distance in each H_2 molecule equals $2.0a_0$). The ground-state restricted Hartree–Fock (RHF) orbitals, ϕ_i , $i = 1–4$, needed to define the \mathcal{M}_0 and \mathcal{M}_0^\perp configurations, are completely determined by the D_{2h} symmetry of the model.

The ground-state RHF configuration,

$$|\Phi_1\rangle = |(\phi_1)^2(\phi_2)^2\rangle, \quad (28)$$

and the exact (FCI) ground state of the P4 model have the 1A_g symmetry. The total dimension of the FCI 1A_g subproblem is 8. Along with $|\Phi_1\rangle$, Eq. (28), there are six 1A_g -symmetric doubly excited configurations relative to $|\Phi_1\rangle$, including the important

$$|\Phi_2\rangle = |(\phi_1)^2(\phi_3)^2\rangle \quad (29)$$

configuration, and one tetraexcited configuration, $|(\phi_3)^2(\phi_4)^2\rangle$ (singly and triply excited configurations relative to $|\Phi_1\rangle$ do not belong to the 1A_g subproblem).

The main attractiveness of the minimum basis set P4 model (aside from the availability of the exact, FCI eigenstates) is the fact that this is a good physical model for testing new ideas in electronic structure. Indeed, by changing the value of the parameter α , we can continuously vary the level of configurational quasidegeneracy of the electronic ground state. For geometries near the square one ($\alpha \simeq 2.0a_0$), the FCI expansion of the ground state is dominated by the RHF configuration $|\Phi_1\rangle$, Eq. (28), and the doubly excited configuration $|\Phi_2\rangle$, Eq. (29). For example, for $\alpha = 2.1a_0$, the coefficients at $|\Phi_1\rangle$ and $|\Phi_2\rangle$ in the FCI expansion of the ground state (1A_g ; in general, μ 1A_g designates the μ th state of the 1A_g symmetry) equal 0.827 and -0.514 , respectively. For larger values of α , the ground state becomes nondegenerate, with $|\Phi_1\rangle$ being the dominant configuration in the corresponding FCI expansion. By changing the value of α , we can also vary the degree of the quasidegeneracy involving the two lowest 1A_g states. For $\alpha \simeq 2.0a_0$, the ground and the first-excited 1A_g states are separated from the rest of the electronic spectrum. As in the case of the ground state, the first-excited 1A_g state is dominated by $|\Phi_1\rangle$ and $|\Phi_2\rangle$. For example, for $\alpha = 2.1a_0$, the coefficients at $|\Phi_1\rangle$ and $|\Phi_2\rangle$ in the FCI expansion of the 2 1A_g state are 0.501 and 0.813, respectively. As α approaches ∞ , the 2 1A_g state separates from the ground state and gains a significant contribution

from other configurations than $|\Phi_1\rangle$ and $|\Phi_2\rangle$. In the $\alpha \rightarrow \infty$ limit, the ground state is completely separated from the rest of the electronic spectrum.

In order to gain an insight into the importance of the model space choice on the structure of multiple solutions of the Bloch equation, we consider the following three model spaces:

- (i) $\mathcal{M}_0^{(1)} = \text{Is}\{|(\phi_1)^2(\phi_2)^2\rangle, |(\phi_1)^2(\phi_3)^2\rangle\} \equiv \text{Is}\{|\Phi_1\rangle, |\Phi_2\rangle\}$; $M = M^{(1)} \equiv \dim \mathcal{M}_0^{(1)} = 2$.
- (ii) $\mathcal{M}_0^{(2)} = \text{Is}\{|(\phi_1)^2(\phi_2)^2\rangle, |(\phi_1)^2(\phi_3)^2\rangle, |(\phi_1)^2(\phi_4)^2\rangle\}$; $M = M^{(2)} \equiv \dim \mathcal{M}_0^{(2)} = 3$.
- (iii) $\mathcal{M}_0^{(3)}$, the model space spanned by $|\Phi_1\rangle$, Eq. (28), and all 1A_g -symmetric doubly excited configurations relative to $|\Phi_1\rangle$; $M = M^{(3)} \equiv \dim \mathcal{M}_0^{(3)} = 7$.

The two-dimensional model space $\mathcal{M}_0^{(1)}$ was used earlier in testing the SUCC approach [9, 10, 14]. From the above discussion it follows that $\mathcal{M}_0^{(1)}$ is a good choice of the reference space for describing the two lowest-energy 1A_g states in the quasidegenerate region ($\alpha \simeq 2.0a_0$). For larger α values, only the ground state has large component in $\mathcal{M}_0^{(1)}$. In this region, the 2 1A_g state is poorly described by the $\mathcal{M}_0^{(1)}$ configurations. As explained in Ref. [9], the $\mathcal{M}_0^{(1)}$ space is a *complete model space* for the 1A_g subproblem. Reference spaces $\mathcal{M}_0^{(2)}$ and $\mathcal{M}_0^{(3)}$ are *incomplete model spaces*. Model space $\mathcal{M}_0^{(3)}$ includes almost all configurations of the FCI 1A_g subproblem. The only configuration of the FCI 1A_g subproblem that is missing in $\mathcal{M}_0^{(3)}$ is the quadruply excited configuration relative to $|\Phi_1\rangle$, i.e., $|(\phi_3)^2(\phi_4)^2\rangle$.

In order to study the effect of the form of the wave operator on the solutions of the Bloch equation, we consider the following two schemes:

- (i) *The exact Bloch formalism* (referred to as the BFCI method), in which all nonvanishing matrix elements U_{kq} , corresponding to the 1A_g FCI subproblem, are included in Eq. (25). In this case, the excitation operators $C^{(q)}$, $q = 1, \dots, M$, that define the wave operator U through Eq. (12), have the exact, FCI-like form of Eq. (13).
- (ii) *The approximate Bloch formalism* (referred to as the BCID approach), in which we consider only those matrix elements U_{kq} , for which the \mathcal{M}_0^\perp configurations $|\Phi_k\rangle$ are doubly excited

with respect to reference configurations $|\Phi_q\rangle$. In this case, the excitation operators $C^{(q)}$ that define U are approximated by the doubly excited components,

$$C^{(q)} \simeq C_2^{(q)}, \quad (q = 1, \dots, M). \quad (30)$$

As in the case of the exact (BFCI) theory, the BCID approach is based on the simplest possible, linear parametrization of the wave operator, although U is no longer exact in this case. Unlike the SUCCD equations, which contain terms that are quartic in $T_2^{(q)}$, the BCID equations contain terms that are at most bilinear in $C_2^{(q)}$. In a sense, the BCID approach can be regarded as an analog of the popular MRCI methods. There are, however, differences between the BCID and MRCI approaches that are worth mentioning here. Let $\mathcal{M}_0^{\perp(q)} \subseteq \mathcal{M}_0^\perp$ be a subspace spanned by configurations that are doubly excited relative to a given $|\Phi_q\rangle$. In the BFCI theory, all $\mathcal{M}_0^{\perp(q)}$ subspaces are identical, i.e., $\mathcal{M}_0^{\perp(q)} = \mathcal{M}_0^\perp$ for every q . However, in the BCID method, the $\mathcal{M}_0^{\perp(q)}$ subspaces corresponding to different values of q are usually different. For example, for the P4 model described by a two-dimensional model space $\mathcal{M}_0^{(1)}$, the $\mathcal{M}_0^{\perp(q=1)}$ subspace is spanned by the configurations $|(\phi_1)^2(\phi_4)^2|$, $|(\phi_2)^2(\phi_3)^2|$, $|(\phi_2)^2(\phi_4)^2|$, and two totally symmetric singlet configurations of the $|(\phi_1)^1(\phi_2)^1(\phi_3)^1(\phi_4)^1|$ type, whereas the $\mathcal{M}_0^{\perp(q=2)}$ subspace is spanned by $|(\phi_1)^2(\phi_4)^2|$, $|(\phi_2)^2(\phi_3)^2|$, $|(\phi_3)^2(\phi_4)^2|$, and two 1A_g configurations of the $|(\phi_1)^1(\phi_2)^1(\phi_3)^1(\phi_4)^1|$ type. The configuration $|(\phi_2)^2(\phi_4)^2| \in \mathcal{M}_0^{\perp(q=1)}$ is not in $\mathcal{M}_0^{\perp(q=2)}$ and $|(\phi_3)^2(\phi_4)^2| \in \mathcal{M}_0^{\perp(q=2)}$ is not in $\mathcal{M}_0^{\perp(q=1)}$. As we will see in Section 5, this asymmetric treatment of the excitation manifolds corresponding to different model space configurations $|\Phi_p\rangle$ in the BCID theory contributes to pathologies observed when solving the Bloch (and related MRCC) equations. In the MRCID (MRCI doubles) method, we would simply define a *single* Q -space

$$\mathcal{M}_{\text{MRCI}}^\perp = \text{ls} \left\{ \bigcup_{q=1}^M \mathcal{M}_0^{\perp(q)} \right\} \subseteq \mathcal{M}_0^\perp \quad (31)$$

and diagonalize the Hamiltonian in the Hilbert subspace $\mathcal{M}_0 \oplus \mathcal{M}_{\text{MRCI}}^\perp$ (in the above example of the P4 model, $\mathcal{M}_{\text{MRCI}}^\perp = \mathcal{M}_0^\perp$, so that the MRCID problem is equivalent in this case to a FCI problem; this should be contrasted by the fact that the BCID and BFCI problems are different). We could recast the MRCID (or any MRCI) eigenvalue prob-

lem for M selected eigenstates of H into the matrix Bloch equation that looks like Eq. (23), provided that the values of j and k in Eq. (23) run over a *single* set of configurations that span $\mathcal{M}_{\text{MRCI}}^\perp$, Eq. (31). Nothing like this is possible in the BCID theory, where the range of j values labeling the matrix elements U_{jp} depends on p (different references $|\Phi_p\rangle$ lead to different ranges of j values, as in the above example of the P4 model described by model space $\mathcal{M}_0^{(1)}$). This fundamental difference between the MRCID and BCID methods results in significant difference between the numbers and types of solutions of the MRCID and BCID equations (see Section 5).

Each solution of the BCID equations can be characterized by the parameter

$$d = \text{tr}(\mathbf{V}^\dagger \mathbf{V}), \quad (32)$$

where

$$\mathbf{V}_{q\mu} = \langle \Phi_q | \Psi_\mu^{\text{BCID}} \rangle, \quad (q, \mu = 1, \dots, M), \quad (33)$$

which provide us with a measure of the proximity between the model space \mathcal{M}_0 and the BCID target space $\mathcal{M}^{\text{BCID}} = \text{ls}\{|\Psi_\mu\rangle\}_{\mu=1}^M$ (cf. Refs. [14, 37]). It can be demonstrated that $0 \leq d \leq M$. Another parameter that can occasionally be useful in identifying and characterizing the solutions of the BCID equations is the parameter

$$\Delta_{\kappa_1 \dots \kappa_M} = \text{tr}(\mathbf{Z}^\dagger \mathbf{Z}), \quad (34)$$

where

$$\begin{aligned} \mathbf{Z}_{\mu\nu} &= \langle \Psi_\mu^{\text{BCID}} | \Psi_\nu^{\text{FCI}} \rangle, \\ (\mu &= 1, \dots, M, \nu = \kappa_1, \dots, \kappa_M; \\ 1 &\leq \kappa_1 < \kappa_2 < \dots < \kappa_M \leq N_C). \end{aligned} \quad (35)$$

The parameter $\Delta_{\kappa_1 \dots \kappa_M}$ provides us with a measure of the proximity between the BCID target space $\mathcal{M}^{\text{BCID}}$ and the FCI target space $\mathcal{M}_{\kappa_1 \dots \kappa_M}^{\text{FCI}} = \text{ls}\{|\Psi_{\kappa_1}^{\text{FCI}}\rangle, \dots, |\Psi_{\kappa_M}^{\text{FCI}}\rangle\}$, spanned by M selected FCI states $|\Psi_{\kappa_i}^{\text{FCI}}\rangle$, $i = 1, \dots, M$. By comparing the values of $\Delta_{\kappa_1 \dots \kappa_M}$ corresponding to different choices of indices $\kappa_1, \dots, \kappa_M$, we can decide which subset of M exact eigenstates of the Hamiltonian is best described by a given solution of the BCID equations. The larger the value of $\Delta_{\kappa_1 \dots \kappa_M}$, the better the description of $\mathcal{M}_{\kappa_1 \dots \kappa_M}^{\text{FCI}}$ that is obtained with a given BCID solution. As in the case of the proximity d , the value of $\Delta_{\kappa_1 \dots \kappa_M}$ cannot exceed M .

Finally, in discussing the results of the BCID calculations, it is useful to characterize the FCI states

by the parameters [14],

$$S_Y^{(\mu)} = \|Y|\Psi_\mu^{\text{FCI}}\|^2, \quad Y = P, Q_C, Q_R. \quad (36)$$

Here, P is a projection operator onto the model space \mathcal{M}_0 [cf. Eq. (7)], Q_C is a projection operator onto the subspace

$$\mathcal{M}_C = \bigcap_{q=1}^M \mathcal{M}_0^{\perp(q)}, \quad (37)$$

where $Q_R = Q - Q_C$ is a projection operator onto $\mathcal{M}_R = \mathcal{M}_0^\perp - \mathcal{M}_C$. Since three different model spaces are considered in this work, we label the quantities $S_Y^{(\mu)}$ by an extra index i specifying the model space $\mathcal{M}_0^{(i)}$ ($i = 1-3$).

5. Results of the Homotopy BFCI and BCID Calculations

We begin our discussion by analyzing the numbers of solutions of the exact and approximate Bloch equations. In the case of the BFCI formalism, the Bloch equation has

$$\binom{N_C}{M} \quad (38)$$

solutions for U , which correspond to all possible ways of selecting M eigenstates $|\Psi_\mu\rangle$ out of all N_C exact states that have nonzero overlap with \mathcal{M}_0 . For the single-reference case, i.e., $M = 1$, we obtain $\binom{N_C}{1} = N_C$ solutions. In this case, each solution U_μ generates the corresponding FCI state $|\Psi_\mu\rangle = U_\mu|\Phi\rangle$, $\mu = 1, \dots, N_C$, where $|\Phi\rangle$ is the reference configuration. When $M = N_C$, i.e., when the model space \mathcal{M}_0 and the N -electron Hilbert space \mathcal{H}_N are identical, the Bloch equation has only $\binom{N_C}{N_C} = 1$ solution U , which describes energies and wave functions of all exact states. In this case, both P and U reduce to the unit operator ($\mathbf{1}$) in \mathcal{H}_N . In consequence, the whole calculation reduces to the diagonalization of the Hamiltonian in \mathcal{H}_N (the FCI problem), since $H^{\text{eff}}(U) = PHUP = H$ when $U = P = \mathbf{1}$. The situation gets more complicated when $1 < M < N_C$. Even for model spaces of rather small dimensions, the Bloch equation can produce a large number of solutions. For example, in the simplest multireference case, when $M = 2$, the Bloch equation has already $\frac{1}{2}N_C(N_C - 1)$ solutions. Each solution describes a pair (Ψ_μ, Ψ_ν) of the FCI states that have nonzero overlaps with \mathcal{M}_0 . For larger values of M , we can obtain even larger numbers of solutions (the largest number of solutions for a given

value N_C , i.e., for a given dimension of the FCI problem, is obtained when $M = \lfloor N_C/2 \rfloor$). The fact that the number of solutions of the exact Bloch equation is given by Eq. (38) may have serious consequences for the practical applications of any theory based on the Bloch wave operator formalism, since, as demonstrated below, the large number of solutions of the exact theory may become even larger when the wave operator U is approximated in some way.

The homotopy BFCI calculations confirm the correctness of Eq. (38). For the minimum basis set P4 model, the BFCI equations corresponding to model spaces $\mathcal{M}_0^{(1)}$, $\mathcal{M}_0^{(2)}$, and $\mathcal{M}_0^{(3)}$ have $\binom{8}{2} = 28$, $\binom{8}{3} = 56$, $\binom{8}{7} = 8$ solutions, respectively.

The BCID homotopy calculations show that in spite of the fact that the BCID approach uses the simplest possible, CI-like (i.e., linear) parametrization for the wave operator U , the numbers of solutions of the Bloch equation increase from 28 in the exact case to 50 in the BCID case, when the model space $\mathcal{M}_0^{(1)}$ is employed, and from 56 in the exact case to 336 in the BCID case, when the model space $\mathcal{M}_0^{(2)}$ is used. Only for the seven-dimensional model space $\mathcal{M}_0^{(3)}$, the number of solutions of the Bloch equation slightly decreases, from 8 in the exact case to 7 in the BCID case. The BCID equations have both real and complex solutions U . In addition, some real solutions lead to effective Hamiltonians that have complex eigenvalues (let us recall that except for $M = 1$ and $M = N_C$, the effective Hamiltonian is not Hermitian and may possess complex eigenvalues).

It is remarkable to observe that in spite of the simplicity of the BCID parametrization of the wave operator, the number of solutions of the BCID equations may significantly exceed the number of solutions of the exact Bloch theory (6-fold, when the $\mathcal{M}_0^{(2)}$ model space is employed). This indicates that even the simplest approximate approaches based on the Bloch formalism may produce large numbers of solutions that have no physical interpretation. The nonlinear parametrization of the wave operator used in the MRCC methods complicates the situation even further [14], but it seems to us that the nonlinearity of the Bloch equation itself is one of the main reasons of the existence of unphysical multiple solutions that plague MRCC calculations [9, 14, 20]. For example, the SUCCD equations for the minimum basis set P4 model employing $\mathcal{M}_0^{(1)}$ as a model space have 133 solutions [14], which clearly is a

large number of solutions (the corresponding FCI problem has only 8 solutions and the BFCI theory gives 28 solutions in this case). We can see, however, that even without using the CC exponential parametrization we may obtain a large number of solutions for the same problem. Indeed, the BCID theory, which is a lot simpler than the SUCCD formalism, gives as many as 50 solutions for the minimum basis set P4 model employing $\mathcal{M}_0^{(1)}$.

The fact that the BCID approach gives usually a much larger number of solutions than the exact (BFCI) theory and that solutions of the BCID equations are often pathological (cf. the discussion below) is related to two factors. The first one is the nonlinearity of the Bloch equation. The second one is the aforementioned asymmetric treatment of the excitation manifolds corresponding to different reference configurations $|\Phi_p\rangle$ in truncated Bloch theories, such as BCID. An asymmetric treatment of the excitation manifolds in the BCID theory causes that the corresponding nonlinear system of equations cannot be recast into any Hermitian eigenvalue problem. This significant distortion of the exact Bloch formalism, resulting from truncating the operators $C^{(q)}$ at $C_2^{(q)}$, results in a nonlinear system that has numerous and often pathological solutions, which would not appear if we kept all excitations in $C^{(q)}$ (the BFCI case) or if we made all subspaces $\mathcal{M}_0^{\perp(q)}$, $q = 1, \dots, M$ identical (the MRCI case). As explained earlier, in the MRCI case we would use a single Q -space $\mathcal{M}_{\text{MRCI}}^{\perp}$, Eq. (31), to define matrix elements U_{jp} of U , and the corresponding Bloch equation would automatically become equivalent to an eigenvalue problem for H in subspace $\mathcal{M}_0 \oplus \mathcal{M}_{\text{MRCI}}^{\perp}$, in which we solve for M selected eigenstates of H . The number of solutions of the Bloch equation, representing the MRCI problem, is given by the formula

$$\binom{N_{\text{MRCI}}}{M}, \quad (39)$$

where $N_{\text{MRCI}} = \dim\{\mathcal{M}_0 \oplus \mathcal{M}_{\text{MRCI}}^{\perp}\}$. This corresponds to all possible ways of selecting M eigenstates out of all N_{MRCI} states that can be obtained by solving the MRCI eigenvalue problem. Since $N_{\text{MRCI}} < N_C$, we automatically must have

$$\binom{N_{\text{MRCI}}}{M} < \binom{N_C}{M}, \quad (40)$$

which implies that, unlike in the BCID case, the number of solutions of the Bloch equation representing the MRCI problem does not exceed the number of BFCI solutions. In addition, each so-

lution of the Bloch equation corresponding to the MRCI eigenvalue problem must be real and represent an approximation to a set of M exact eigenstates of H . The solutions of the BCID equations do not have to possess this property. The nonlinear character of the BCID equations, combined with the asymmetric treatment of the excitation manifolds corresponding to different references, leads to real as well as complex or pathological solutions that usually significantly outnumber the solutions of the exact BFCI problem. Essentially, the same remarks apply to all existing genuine MRCC theories. Indeed, all MRCC equations are nonlinear. In addition, in the existing SUCCD and SUCCSD (SUCC singles and doubles) methods [6–16], the excitation manifolds used to define cluster operators $T^{(p)}$ for different references $|\Phi_p\rangle$ are not identical. A symmetric treatment of the excitation manifolds used to define the $T^{(p)}$ operators via, for example, inclusion of semi-internal triples and quadruples in the SUCCSD theory [5], would likely eliminate some of the pathologies that plague the existing SUCC methods, although it would also lead to an increase of computer costs of the SUCC calculations. The SUCC methods with symmetric treatment of the excitation manifolds used to define $T^{(p)}$'s would be closer, in spirit, to the existing MRCI methods and some state-selective CC theories employing semi-internal triples and quadruples [38].

The energies $\Delta E_{\mu}^{\text{BCID}}$ corresponding to all real solutions of the BCID equations giving real energies for the P4 model system with two representative values of α , $\alpha = 2.1a_0$ and $\alpha = 6.0a_0$, are given in Tables I–V. Tables I and II correspond to model space $\mathcal{M}_0^{(1)}$, whereas Tables III and IV correspond to model space $\mathcal{M}_0^{(2)}$. Table V contains the results for model space $\mathcal{M}_0^{(3)}$. Information about the multiconfigurational structure of the exact wave functions $|\Psi_{\mu}^{\text{FCI}}\rangle \equiv |\mu \ ^1A_g\rangle$, as described by the parameters $S_Y^{(\mu)}$, Eq. (36), and information about the corresponding FCI energies $\Delta E_{\mu}^{\text{FCI}}$ are given in Table VI.

The results in Table I show that in the quasidegenerate region there is only one solution of the BCID equations (designated in Tables I and II by A) that has a large proximity d with the model space $\mathcal{M}_0^{(1)}$ (for $\alpha = 2.1a_0$, $d = 1.871$; $d = 2.0$ would be the maximum value of d in this case). The remaining solutions of the BCID equations are characterized by much smaller d values. Solution A represents the standard physical solution of the BCID equations. It describes the ground and the first-excited states, for

TABLE I
BCID energies $\Delta E_{\mu}^{\text{BCID}} = E_{\mu}^{\text{BCID}} - \langle \Phi_1 | H | \Phi_1 \rangle$, $\mu = 1, 2$ (in mhartree), and the proximities d between the model space \mathcal{M}_0 and the BCID target spaces $\mathcal{M}^{\text{BCID}}$, Eq. (32), corresponding to all real solutions of the BCID equations with real energies for the minimum basis set P4 model with $\alpha = 2.1a_0$ and $\mathcal{M}_0 = \mathcal{M}_0^{(1)}$ ($M = 2$).

Sol. No.	ΔE_1^{BCID}	ΔE_2^{BCID}	d	Sol. No.	ΔE_1^{BCID}	ΔE_2^{BCID}	d
1	-199.144	1275.053	0.456	22	184.928	942.260	0.069
2	-140.598	1277.687	0.766	23	414.692	1943.531	0.058
3(B)	-116.264	659.568	0.954	24	419.320	1977.724	0.043
4(C)	-99.973	942.462	0.940	25	591.805	942.429	0.064
5(A)	-92.127	28.523	1.871	26	663.092	1263.034	0.088
6	-46.323	3424.874	0.000	27	676.689	1282.938	0.089
7(D)	-20.240	1083.074	0.514	28	687.282	1201.508	0.111
8	-4.281	1878.417	0.513	29	716.469	1306.113	0.080
9	6.965	942.442	0.526	30	720.644	942.484	0.060
10	7.259	624.911	0.704	31	766.903	942.624	0.041
11	13.122	1280.554	0.781	32	942.164	2534.906	0.000
12	16.122	719.108	0.448	33	942.362	1852.779	0.003
13	19.921	1306.440	0.446	34	942.436	1908.070	0.002
14(F)	23.567	1190.264	0.722	35	942.461	1267.426	0.016
15	23.658	942.474	0.821	36	942.487	1181.154	0.047
16	39.038	1259.946	0.866	37	942.495	1284.931	0.022
17(E)	42.055	637.718	0.882	38	942.558	1342.002	0.022
18	60.082	942.366	0.471	39	1082.854	2328.516	0.000
19	62.055	1855.684	0.484	40	1220.225	1284.132	0.059
20	133.459	942.187	0.157	41	1375.641	1613.608	0.028
21(G)	143.388	984.098	0.113	42	1384.786	1624.575	0.021

which the model space $\mathcal{M}_0^{(1)}$ provides a very good zero-order approximation (see the values of $S_{p_1}^{(\mu)}$ in Table VI; cf., also discussion in Section 4). For larger α values, the model space $\mathcal{M}_0^{(1)}$ is no longer capable of providing a reasonable description of the target space spanned by the 1 1A_g and 2 1A_g states (cf. the $S_{p_1}^{(\mu)}$ values in Table VI). Indeed, as α assumes larger values, the proximity d of the physical solution A with the model space $\mathcal{M}_0^{(1)}$ significantly decreases (from $\simeq 2.0$ at $\alpha \simeq 2.0a_0$ to 1.230 for $\alpha = 6.0a_0$; see Table II). In consequence, the BCID energies become a poorer representation of the exact energies ΔE_1^{FCI} and ΔE_2^{FCI} for larger α values. The BCID results obtained with solution A are particularly poor for the first-excited state. The very small, 0.572 mhartree, difference between ΔE_2^{BCID} and ΔE_2^{FCI} for $\alpha = 2.1a_0$ (cf. Tables I and VI) increases to 88.673 mhartree for $\alpha = 6.0a_0$ (cf. Tables II and VI). As a matter of fact, there are other solutions of the BCID equations that can provide better description of either the ground state or the first-excited state in the region of large α values. For example, the BCID solutions that are designated in Tables I and II as solutions B, C, and D

(particularly B and D) provide better description of the ground state for $\alpha = 6.0a_0$ than the physical solution A (the difference between ΔE_1^{BCID} and ΔE_1^{FCI} for solution A is 4.625 mhartree; in the case of solutions B and D, the differences between ΔE_1^{BCID} and ΔE_1^{FCI} do not exceed 2 mhartree). For $\alpha = 6.0a_0$, these solutions describe the following states: the ground state and state 3 1A_g (solution B), the ground state and state 5 1A_g (solution C), and the ground state and state 6 1A_g (solution D). In the region of larger α values, the proximities d characterizing solutions B, C, and D are comparable with the values of d characterizing solution A. In fact, the value of d characterizing solution B at $\alpha = 6.0a_0$ is larger than the corresponding value of d characterizing the physical solution A ($d = 1.411$ for solution B and 1.230 for solution A; cf. Table II). This is related to the fact that state 3 1A_g , described by solution B, has a larger $\mathcal{M}_0^{(1)}$ component than state 2 1A_g , described by solution A (see the values of $S_{p_1}^{(\mu)}$ in Table VI). Other solutions of the BCID equations are worth mentioning here, too. The solutions labeled in Tables I and II by letters E, F, and G (particu-

TABLE II
BCID energies $\Delta E_{\mu}^{\text{BCID}} = E_{\mu}^{\text{BCID}} - \langle \Phi_1 | H | \Phi_1 \rangle$, $\mu = 1, 2$ (in mhartree), and the proximities d between the model space \mathcal{M}_0 and the BCID target spaces $\mathcal{M}^{\text{BCID}}$, Eq. (32), corresponding to all real solutions of the BCID equations with real energies for the minimum basis set P4 model with $\alpha = 6.0a_0$ and $\mathcal{M}_0 = \mathcal{M}_0^{(1)}$ ($M = 2$).

Sol. No.	ΔE_1^{BCID}	ΔE_2^{BCID}	d	Sol. No.	ΔE_1^{BCID}	ΔE_2^{BCID}	d
1	-2438.776	1085.642	0.001	21(E)	492.438	921.089	0.809
2	-145.937	1089.958	0.205	22	493.596	1080.122	0.253
3	-85.714	2726.231	0.000	23	548.961	1002.328	0.290
4	-62.337	1805.150	1.072	24	810.338	1001.851	0.054
5(B)	-53.868	825.325	1.411	25	816.239	1787.908	0.225
6(D)	-53.093	1060.003	1.090	26	844.945	1059.778	0.318
7(C)	-50.236	1002.192	0.950	27	854.835	1002.678	0.581
8(A)	-50.215	557.564	1.230	28	925.100	1079.861	0.572
9	-38.793	1669.017	0.894	29	948.439	1947.181	0.592
10	-32.032	1002.135	0.209	30	986.727	1006.461	0.676
11	90.250	1001.921	0.161	31	999.994	1038.136	0.392
12	113.501	823.103	0.158	32	1000.978	1571.401	0.005
13	195.626	431.052	0.112	33	1001.743	1782.429	0.160
14	253.313	1809.223	0.142	34	1002.058	1755.991	0.101
15	323.469	1002.166	0.022	35	1002.371	2073.893	0.017
16	341.936	1739.243	0.263	36	1003.485	1078.831	0.025
17	357.215	1738.760	0.209	37	1005.166	1938.946	0.180
18(G)	452.566	1060.822	0.271	38	1089.778	1593.801	0.097
19	469.512	1937.710	0.334				
20(F)	479.185	1003.770	0.250				

larly, solution F) provide better description of the first-excited state for $\alpha = 6.0a_0$ than the physical solution A. These solutions describe the following pairs of states at $\alpha = 6.0a_0$: 2^1A_g and 3^1A_g (solution E; cf. Section 6 for additional comments), 2^1A_g and 5^1A_g (solution F), and 2^1A_g and 6^1A_g (solution G). The proximities d characterizing solutions E, F, and G are smaller than in the case of solutions B, C, and D, although the value of d for solution E remains close to 1.0. The relatively large value of d for solution E that describes the pair of 2^1A_g and 3^1A_g states is a consequence of the fact that state 2^1A_g and state 3^1A_g have relatively large $\mathcal{M}_0^{(1)}$ components (see the values of $S_{P_1}^{(\mu)}$ in Table VI).

The dependencies of energies $\Delta E_{\mu}^{\text{BCID}}$, $\mu = 1, 2$, corresponding to solutions A, B, C, and D and A, E, F, and G on the parameter α are shown in Figures 1 and 2, respectively. Figure 1 clearly shows that there is a number of solutions of the BCID equations that can provide excellent description of state 1^1A_g . Figure 2 shows that there are a few solutions of the BCID equations that can provide better description of state 2^1A_g than solution A. Some solutions, such as the physical solution A and so-

lution B, seem to represent the same pair of energies for all values of α [$(\Delta E_1^{\text{FCI}}, \Delta E_2^{\text{FCI}})$ in the case of solution A and $(\Delta E_1^{\text{FCI}}, \Delta E_3^{\text{FCI}})$ in the case of solution B]. Some other solutions describe one pair of energies for larger α values and another pair for small values of α . A good example of such a situation is provided by solution C. Solution C describes a pair $(\Delta E_1^{\text{FCI}}, \Delta E_5^{\text{FCI}})$ for large α 's and $(\Delta E_1^{\text{FCI}}, \Delta E_4^{\text{FCI}})$ for intermediate and small α values. An interesting situation is produced by solution F. This solution has a singularity (a pole) at $\alpha = 4.01a_0$: the matrix elements U_{k1} become infinitely large at $\alpha \simeq 4.01a_0$ and change sign from the large positive to large negative values as we proceed from $\alpha > 4.01a_0$ to $\alpha < 4.01a_0$. At the same time, matrix elements U_{k2} remain finite at $\alpha = 4.01a_0$ and the off-diagonal element $H_{12}^{\text{eff}}(U)$ approaches 0 as $\alpha \rightarrow 4.01a_0$. The eigenvalues of $H^{\text{eff}}(U)$ [$H_{11}^{\text{eff}}(U)$ and $H_{22}^{\text{eff}}(U)$ in this case] remain finite at $\alpha = 4.01a_0$, so that the singularity of the solution U does not result in the singular behavior of the eigenvalues of $H^{\text{eff}}(U)$.

It is interesting to observe that one of the two energies provided by solution C in the quasidegenerate region is almost identical to ΔE_4^{FCI} , in spite of

TABLE III

BCID energies $\Delta E_{\mu}^{\text{BCID}} = E_{\mu}^{\text{BCID}} - \langle \Phi_1 | H | \Phi_1 \rangle$, $\mu = 1, 2, 3$ (in mhartree), and the proximities d between the model space \mathcal{M}_0 and the BCID target spaces $\mathcal{M}^{\text{BCID}}$, Eq. (32), corresponding to all real solutions of the BCID equations with real energies for the minimum basis set P4 model with $\alpha = 2.1a_0$ and $\mathcal{M}_0 = \mathcal{M}_0^{(2)}$ ($M = 3$).

Sol. No.	ΔE_1^{BCID}	ΔE_2^{BCID}	ΔE_3^{BCID}	d	Sol. No.	ΔE_1^{BCID}	ΔE_2^{BCID}	ΔE_3^{BCID}	d
1	-3885.322	-189.657	1265.890	0.497	36	21.288	1123.926	1793.898	0.866
2	-818.762	23.374	1034.151	0.070	37	25.517	788.584	1321.218	1.411
3	-531.902	-531.902	1475.632	0.066	38	27.277	613.671	1117.611	1.552
4(III)	-249.139	-48.716	1104.879	0.906	39	28.122	884.627	1336.954	1.279
5	-222.997	12.871	1096.177	0.945	40	30.342	646.289	1238.037	1.488
6	-209.548	718.587	1676.085	0.551	41	31.037	741.880	1334.911	1.012
7	-199.257	1275.547	1681.510	0.513	42	36.367	800.841	1192.152	1.161
8	-196.203	1236.961	1271.120	1.143	43	46.609	749.450	1305.016	1.423
9	-195.326	3.350	1268.887	0.936	44	47.787	972.767	2064.701	0.182
10	-194.559	846.933	1268.883	0.874	45	55.038	1023.552	1787.691	0.591
11	-193.105	896.370	1265.998	0.937	46	57.090	621.740	1850.819	0.738
12	-190.870	1260.659	1725.697	0.527	47	61.542	305.225	1145.522	0.233
13	-183.289	652.818	1647.222	0.498	48	78.065	647.364	1303.304	0.685
14	-179.570	703.927	1484.650	0.711	49	93.520	717.002	1026.024	0.520
15	-119.145	510.732	1733.039	0.610	50	96.967	1002.826	2296.065	0.094
16	-117.018	1133.288	1757.213	0.899	51	102.022	978.851	2025.960	0.173
17	-115.942	1145.034	1752.640	0.810	52	123.292	976.843	2008.597	0.174
18	-100.855	641.698	1232.689	1.515	53	136.119	986.562	1270.670	0.500
19	-96.618	625.546	1120.324	1.154	54	145.307	996.627	1207.778	0.727
20(I)	-94.511	22.138	1198.015	2.445	55	187.966	884.478	1984.424	0.242
21(II)	-93.792	37.759	782.451	2.315	56	209.607	1054.655	1927.803	0.250
22	-59.896	7.525	1835.726	1.770	57	245.793	245.793	955.501	0.162
23	-41.295	1250.592	1659.116	0.519	58	251.269	1062.319	1986.420	0.179
24	-38.140	1082.310	4340.640	0.100	59	332.185	332.185	1906.026	0.312
25	-32.107	1082.913	1259.098	1.038	60	401.894	401.894	1792.668	0.386
26	-30.523	1264.888	1679.110	0.602	61	515.498	1083.400	1893.934	0.274
27	-27.927	778.632	1087.090	0.956	62	678.713	1195.068	1262.095	0.661
28	-17.003	1111.929	1835.894	0.750	63	708.733	1268.144	1709.274	0.195
29	-16.593	683.374	1331.561	0.921	64	709.643	1270.399	1689.840	0.224
30	-6.620	1151.563	1774.174	0.882	65	854.264	1571.772	1571.772	0.031
31	-4.546	1099.576	1872.967	0.858	66	872.371	1362.823	1652.512	0.775
32	-2.082	821.632	1822.382	0.582	67	876.115	1386.772	1647.023	0.704
33	3.371	597.816	1084.364	1.384	68	1096.889	2492.008	4308.687	0.001
34	10.449	58.809	941.216	1.006	69	1101.321	2303.294	42248.703	0.000
35	30.342	646.289	1238.037	1.488					

the fact that the fourth state of the 1A_g symmetry is virtually orthogonal to $\mathcal{M}_0^{(1)}$ for $\alpha \simeq 2.0a_0$ (cf. Table VI). There are, in fact, several solutions of the BCID equations that very accurately approximate the energy of the 4 1A_g state (to within 0.3 mhartree) in the $\alpha \simeq 2.0a_0$ region (see Table I and Figs. 1 and 2). There are also a few solutions of the BCID equations that quite accurately describe the energy of the 3 1A_g state (to within 10–20 mhartree) in the region of small α values (including solutions B and E; see

Table I and Figs. 1 and 2), in spite the fact that Ψ_3^{FCI} has a very small $\mathcal{M}_0^{(1)}$ component for $\alpha \simeq 2.0a_0$.

As we can see, the BCID theory has many solutions U that very accurately approximate energies of these eigenstates of the Hamiltonian that are virtually orthogonal to the model space. A very similar behavior has recently been observed in the context of SUCCD calculations [14]. Many solutions of the SUCCD equations provide energies of eigenstates that are almost orthogonal to \mathcal{M}_0 , too. This un-

TABLE IV

BCID energies $\Delta E_{\mu}^{\text{BCID}} = E_{\mu}^{\text{BCID}} - \langle \Phi_1 | H | \Phi_1 \rangle$, $\mu = 1, 2, 3$ (in mhartree), and the proximities d between the model space \mathcal{M}_0 and the BCID target spaces $\mathcal{M}^{\text{BCID}}$, Eq. (32), corresponding to all real solutions of the BCID equations with real energies for the minimum basis set P4 model with $\alpha = 6.0a_0$ and $\mathcal{M}_0 = \mathcal{M}_0^{(2)}$ ($M = 3$).

Sol. No.	ΔE_1^{BCID}	ΔE_2^{BCID}	ΔE_3^{BCID}	d	Sol. No.	ΔE_1^{BCID}	ΔE_2^{BCID}	ΔE_3^{BCID}	d
1	-1838.140	-12.452	1111.580	0.203	41	108.110	1063.991	1780.759	0.344
2	-1336.195	-8.263	1075.831	0.139	42	112.640	1076.156	1778.832	0.371
3	-847.118	1116.515	1628.890	0.061	43	153.736	473.059	1777.693	0.200
4	-786.073	1114.635	1755.984	0.055	44	232.880	813.345	1064.914	0.515
5	-321.682	1112.062	1685.725	0.046	45	291.251	1127.450	1483.699	0.219
6	-250.279	1151.837	1467.961	0.138	46	304.888	1073.737	1611.991	0.750
7	-248.367	1154.864	1463.937	0.121	47	307.026	816.708	1075.561	0.560
8	-244.793	1111.666	1660.534	0.070	48	316.872	1057.556	1649.480	1.056
9	-231.401	1166.330	1444.060	0.162	49	329.472	815.412	1772.532	0.855
10	-231.032	22.001	1737.319	0.462	50	330.620	797.374	1779.944	0.916
11	-217.684	1076.071	1411.322	0.159	51	338.880	1078.143	1558.235	0.583
12	-184.973	1132.946	1472.364	0.224	52	369.696	1100.560	1193.699	0.455
13	-171.810	122.574	1519.181	0.365	53	432.486	1053.034	1130.064	0.704
14	-163.843	959.478	1129.618	0.244	54	440.202	1051.798	1916.503	0.890
15	-144.947	931.015	1127.467	0.276	55	442.388	1056.708	1918.113	1.069
16	-91.432	1074.988	1681.312	0.924	56	445.025	1021.769	1064.626	1.099
17	-84.125	473.125	1689.484	1.030	57	452.736	1053.437	1307.225	0.520
18	-81.957	457.609	1717.511	1.079	58	454.360	1066.448	1929.378	0.530
19	-79.827	716.776	1233.369	0.986	59	456.306	1020.569	1069.692	0.935
20	-76.744	1076.600	1707.863	1.200	60	456.388	1067.018	1834.766	0.498
21	-58.718	483.070	1580.737	1.188	61	456.576	847.618	1020.547	1.088
22	-56.640	800.664	995.780	1.773	62	483.910	965.683	988.963	1.402
23	-56.623	1071.320	1555.292	1.315	63	500.607	919.676	1083.495	1.133
24	-55.015	794.445	1911.565	1.566	64	500.754	939.473	1956.775	1.181
25(III)	-54.747	402.824	1065.052	1.459	65	609.918	1076.213	1748.386	0.339
26(IV)	-54.648	464.624	1606.768	1.201	66	709.460	1093.297	2013.463	0.858
27	-54.311	1076.918	1593.657	1.374	67	755.051	1068.303	1689.453	0.358
28	-54.080	833.842	1071.085	1.760	68	756.803	799.731	1596.110	0.302
29(I)	-54.070	464.315	1072.128	1.525	69	761.241	861.176	2007.354	1.145
30	-53.317	854.655	1063.534	1.645	70	824.678	1074.244	1592.237	0.574
31	-53.190	1019.314	1072.193	1.519	71	829.944	1103.661	1874.955	0.712
32	-52.191	1074.750	3066.708	0.215	72	848.585	1018.420	1073.570	0.842
33(II)	-51.885	528.521	915.655	2.108	73	900.915	1099.631	1574.289	0.801
34	-31.450	759.553	1683.303	1.214	74	916.718	1106.028	1265.891	0.770
35	-26.053	1053.212	2797.451	0.258	75	938.003	1062.112	1940.058	1.086
36	-22.565	640.688	1236.380	0.927	76	952.226	1030.790	1939.906	1.241
37	0.408	1725.791	4218.715	0.510	77	1009.838	1205.765	1419.531	0.325
38	3.633	597.646	1249.278	0.729	78	1015.137	1078.723	1531.717	0.332
39	21.017	745.107	1108.048	0.416	79	1049.469	1089.759	1501.383	0.301
40	102.556	610.494	876.568	0.828					

usual behavior of the BCID and SUCCD theories is a consequence of the following theorem (proved in Ref. [14]):

Theorem. If $|\Psi_{\mu}\rangle$ is an exact solution of the Schrödinger equation and E_{μ} is its energy and if, for a given

solution U of the Bloch equation (9), not all components of the vector $\mathbf{y}_{\mu} = (y_{\mu,1}, \dots, y_{\mu,M})$, $y_{\mu,p} = \langle \Psi_{\mu} | U | \Phi_p \rangle$, equal zero, then E_{μ} is an eigenvalue and \mathbf{y}_{μ} is the left eigenvector of the effective Hamiltonian $H^{\text{eff}}(U)$. If, in addition, an exact eigenstate $|\Psi_{\mu}\rangle$ satisfies the condition $Q_C |\Psi_{\mu}\rangle = |\Psi_{\mu}\rangle$, where Q_C is a projection operator onto

TABLE V

BCID energies $\Delta E_{\mu}^{\text{BCID}} = E_{\mu}^{\text{BCID}} - \langle \Phi_1 | H | \Phi_1 \rangle$, $\mu = 1-7$ (in mhartree), and the proximities d between the model space \mathcal{M}_0 and the BCID target spaces $\mathcal{M}^{\text{BCID}}$, Eq. (32), corresponding to all solutions of the BCID equations for the minimum basis set P4 model with $\alpha = 2.1a_0$ and $\alpha = 6a_0$ and $\mathcal{M}_0 = \mathcal{M}_0^{(3)}$ ($M = 7$).

Sol. No.	ΔE_1^{BCID}	ΔE_2^{BCID}	ΔE_3^{BCID}	ΔE_4^{BCID}	ΔE_5^{BCID}	ΔE_6^{BCID}	ΔE_7^{BCID}	d
$\alpha = 2.1a_0$								
1	-99.738	28.453	646.829	942.456	1115.674	1238.430	1760.133	6.358
2	-96.788	28.078	645.212	942.456	1112.072	1237.551	1838.303	6.326
3	-70.215	23.820	630.432	942.454	1232.133	1762.269	1864.245	6.448
4	-76.581	25.012	633.982	942.454	1088.874	1761.960	1858.524	6.284
5	50.078	50.078	504.451	961.356	1223.234	1764.785	1970.962	3.335
	-i53.775	+i53.775						
6	-50.229	19.043	942.452	1063.617	1229.857	1762.957	1880.067	3.620
7	-4.905	603.764	942.450	1040.778	1227.729	1763.569	1899.465	5.359
$\alpha = 6.0a_0$								
1	-63.346	468.891	817.820	986.223	1006.316	1076.274	1656.354	6.531
2	-56.486	468.891	804.243	986.010	1006.289	1076.084	1937.296	6.866
3	-46.587	468.891	785.132	985.760	1075.852	1673.225	1937.296	6.745
4	-37.329	468.891	767.748	985.573	1006.234	1681.744	1937.296	6.198
5	-33.397	468.891	761.557	1006.227	1075.612	1684.704	1937.296	4.732
6	-26.901	468.891	985.400	1006.213	1075.499	1690.732	1937.296	4.159
7	-4.666	709.798	985.125	1006.179	1075.213	1707.991	1937.296	5.767

\mathcal{M}_C , Eq. (37), i.e., $|\Psi_{\mu}\rangle \in \mathcal{M}_C \subseteq \mathcal{M}_0^{\perp}$, then the solution of the projected Bloch equation,

$$Q^{(p)}HU|\Phi_p\rangle = Q^{(p)}UHU|\Phi_p\rangle, \quad (p = 1, \dots, M), \quad (41)$$

or

$$Q^{(p)}HU|\Phi_p\rangle = \sum_{q=1}^M Q^{(p)}U|\Phi_q\rangle H_{qp}^{\text{eff}}(U), \quad (42)$$

where $Q^{(p)}$ is a projection operator onto the subspace $\mathcal{M}_0^{(p)} = Q^{(p)}\mathcal{M}_0^{\perp} \subseteq \mathcal{M}_0^{\perp}$ spanned by configurations ${}^{(p)}G_{I(i)}|\Phi_p\rangle$, gives the exact energy E_{μ} of this $|\Psi_{\mu}\rangle$.

There are two important consequences of the above theorem: (i) On the basis of the first part of the theorem we can expect that if U is one of the numerous approximate solutions of the Bloch equation, obtained, for example, by solving BCID or SUCCD equations, then the diagonalization of the corresponding effective Hamiltonian $H^{\text{eff}}(U)$ may produce a nearly exact eigenvalue E_{μ} , in spite of the fact that none of the wave functions provided by this U approximates the exact eigenstate $|\Psi_{\mu}\rangle$. It is true that the first part of the theorem applies, strictly speaking, only to the exact Bloch equation, in which case each of the $\binom{N_C}{M}$ solutions of the exact theory

yields M exact eigenstates of H . However, the first part of the theorem is formulated in terms of vector \mathbf{y}_{μ} , whose components are simple overlaps of the exact state $|\Psi_{\mu}\rangle$ and nonorthogonal states $U|\Phi_p\rangle$, $p = 1, \dots, M$, that span the corresponding target space \mathcal{M} . The condition that not all components of vector \mathbf{y}_{μ} vanish is a rather weak condition that can be satisfied by many solutions of the approximate Bloch equation, not only by the physical ones representing a given set of M eigenstates of H [14]. It is, therefore, not unreasonable to expect (by the virtue of a "good faith" argument) that some solutions of the approximate Bloch equation, for which $\mathbf{y}_{\mu} \neq \mathbf{0}$ for a given μ , give a nearly exact eigenvalue E_{μ} , in spite of the fact that the corresponding U does not describe $|\Psi_{\mu}\rangle$. (ii) On the basis of the second part of the theorem, we can expect that some solutions of the approximate Bloch equation, obtained, for example, by solving the SUCCD or BCID equations, may lead to effective Hamiltonians whose diagonalization gives nearly exact energies E_{μ} of eigenstates $|\Psi_{\mu}\rangle$ that are orthogonal to \mathcal{M}_0 (belong to $\mathcal{M}_C \subseteq \mathcal{M}_0^{\perp}$). This is precisely what we observe in the BCID calculations reported here and SUCCD calculations reported in Ref. [14]. As we can see from Table I, there are at least 16 real solutions of

TABLE VI

Energies $\Delta E_{\mu}^{\text{FCI}} = E_{\mu}^{\text{FCI}} - \langle \Phi_1 | H | \Phi_1 \rangle$ (in mhartree) and the parameters $S_Y^{(\mu)}$, $Y = P_i, Q_{C_i}, Q_{R_i}$, $i = 1, 2, 3$, Eq. (36), characterizing the FCI states $\mu \ ^1A_g = |\Psi_{\mu}^{\text{FCI}}\rangle$ of the P4 model system with $\alpha = 2.1a_0$ and $6.0a_0$.^a

Geometry	Ψ_{μ}^{FCI}							
	1 1A_g	2 1A_g	3 1A_g	4 1A_g	5 1A_g	6 1A_g	7 1A_g	8 1A_g
$\alpha = 2.1a_0$								
$S_{P_1}^{(\mu)}$	0.94860	0.91116	0.07224	0.00017	0.05072	0.01118	0.00128	0.00464
$S_{Q_{C_1}}^{(\mu)}$	0.04722	0.08850	0.90261	0.99982	0.78415	0.91436	0.17359	0.08975
$S_{Q_{R_1}}^{(\mu)}$	0.00418	0.00035	0.02514	0.00001	0.16513	0.07445	0.82513	0.90561
$S_{P_2}^{(\mu)}$	0.94977	0.94153	0.16344	0.45264	0.05247	0.38298	0.00537	0.05179
$S_{Q_{C_2}}^{(\mu)}$	0.04447	0.01440	0.42319	0.10283	0.78228	0.45567	0.16686	0.01030
$S_{Q_{R_2}}^{(\mu)}$	0.00380	0.04397	0.40113	0.44453	0.08649	0.13595	0.58658	0.29755
$S_{P_3}^{(\mu)}$	0.99804	0.99991	0.98775	0.99999	0.92124	0.97460	0.75881	0.35964
$S_{Q_{C_3}}^{(\mu)}$	0.00000	0.00000	0.00000	0.00000	0.00000	0.00000	0.00000	0.00000
$S_{Q_{R_3}}^{(\mu)}$	0.00196	0.00009	0.01225	0.00000	0.07876	0.02540	0.24119	0.64036
Energy	-95.815	27.951	644.678	942.456	1110.895	1237.277	1760.554	1839.345
$\alpha = 6.0a_0$								
$S_{P_1}^{(\mu)}$	0.94531	0.21871	0.23397	0.36093	0.10493	0.01480	0.00655	0.11479
$S_{Q_{C_1}}^{(\mu)}$	0.04695	0.62156	0.63357	0.23818	0.79848	0.86272	0.04974	0.74880
$S_{Q_{R_1}}^{(\mu)}$	0.00774	0.15974	0.13246	0.40089	0.09659	0.12248	0.94371	0.13640
$S_{P_2}^{(\mu)}$	0.95362	0.40354	0.32540	0.49527	0.46741	0.09927	0.01506	0.24042
$S_{Q_{C_2}}^{(\mu)}$	0.03086	0.24852	0.43432	0.02243	0.01146	0.72161	0.03179	0.49901
$S_{Q_{R_2}}^{(\mu)}$	0.01450	0.34793	0.18074	0.48102	0.52076	0.17761	0.01686	0.26058
$S_{P_3}^{(\mu)}$	0.99898	0.99999	0.94046	0.99872	0.99964	0.99849	0.06371	0.99999
$S_{Q_{C_3}}^{(\mu)}$	0.00000	0.00000	0.00000	0.00000	0.00000	0.00000	0.00000	0.00000
$S_{Q_{R_3}}^{(\mu)}$	0.00102	0.00000	0.05954	0.00128	0.00036	0.00151	0.93629	0.00000
Energy	-54.840	468.891	801.027	985.964	1006.283	1076.042	1665.164	1937.296

^a P_1 , P_2 , and P_3 are the projection operators on the three reference spaces considered in this work, $\mathcal{M}_0^{(1)}$, $\mathcal{M}_0^{(2)}$, and $\mathcal{M}_0^{(3)}$, respectively, Q_{C_i} and Q_{R_i} , $i = 1, 2, 3$, are the corresponding operators Q_C and Q_R (see text for details).

the BCID equations giving the energy of state 4 1A_g to within 0.3 mhartree, in spite of the fact that $|\Psi_4^{\text{FCI}}\rangle$ essentially belongs to \mathcal{M}_C for $\alpha \simeq 2.0a_0$ (at $\alpha = 2.1a_0$, $S_{Q_{C_1}}^{(\mu)} = 0.99982$; cf. Table VI). Solution C discussed earlier is one of these solutions. Practically all of these solutions lack physical interpretation and provide very poor representation of $|\Psi_4^{\text{FCI}}\rangle$ in the quasi-degenerate region or, in fact, completely unphysical wave functions, in spite of providing excellent description of the energy of state $|\Psi_4^{\text{FCI}}\rangle$ for smaller

α values. The fact that so many solutions giving the energy of state 4 1A_g are unphysical becomes obvious when we realize that the exact Bloch formalism employing $\mathcal{M}_0^{(1)}$ gives only seven solutions describing $|\Psi_4^{\text{FCI}}\rangle$ (for additional remarks about the physical interpretation of multiple solutions of the BCID equations, see the discussion in the next section). The number of unphysical solutions of the SUCCD equations that approximate the energy of state $|\Psi_4^{\text{FCI}}\rangle$, but not the corresponding wave function, is virtually identical to the number of similar

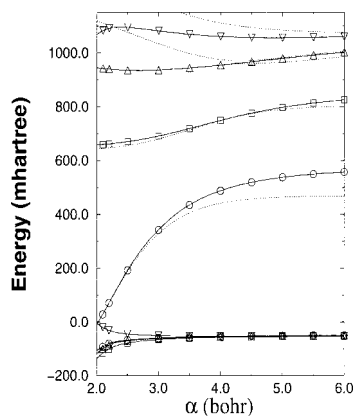


FIGURE 1. Dependence of BCID energies $\Delta E_{\mu}^{\text{BCID}} = E_{\mu}^{\text{BCID}} - \langle \Phi_1 | H | \Phi_1 \rangle$, $\mu = 1, 2$ (in mhartree), on the parameter α (in a_0) for selected solutions of the BCID equations for the minimum basis set P4 model corresponding to the two-dimensional model space $\mathcal{M}_0^{(1)}$. The solutions A, B, C, and D are marked by \circ , \square , \triangle , and ∇ , respectively. Dotted lines represent FCI states of 1A_g symmetry.

solutions of the BCID equations. This implies that the existence of such unusual solutions is a consequence of using the Bloch formalism and not so much the result of assuming a particular (CI-like or CC-like) approximate form of U .

It has been shown in Ref. [14] that solutions of the SUCCD equations, which yield one or more en-

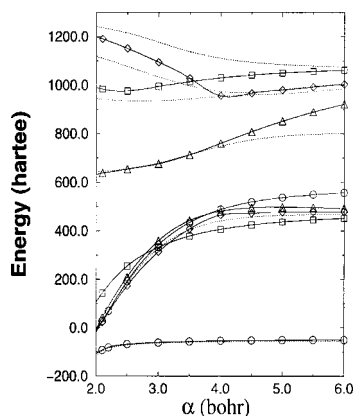


FIGURE 2. Dependence of BCID energies $\Delta E_{\mu}^{\text{BCID}} = E_{\mu}^{\text{BCID}} - \langle \Phi_1 | H | \Phi_1 \rangle$, $\mu = 1, 2$ (in mhartree), on the parameter α (in a_0) for selected solutions of the BCID equations for the minimum basis set P4 model corresponding to the two-dimensional model space $\mathcal{M}_0^{(1)}$. The solutions A, E, F, and G are marked by \circ , \triangle , \diamond , and \square , respectively. Dotted lines represent FCI states of 1A_g symmetry.

ergies of states that have small overlaps with \mathcal{M}_0 in the quasidegenerate region, are responsible for the emergence of the intruder solution problem in SUCCD calculations. In analogy to the intruder state problem of the MRMBPT theory, the intruder solution problem may cause difficulties with converging the desired physical solution in the nondegenerate region. Unphysical solutions of truncated SUCC equations that are characterized by the small proximity d with \mathcal{M}_0 in the quasidegenerate region may evolve into solutions having large proximities with \mathcal{M}_0 in the nondegenerate region (as large as those characterizing the physical solution). The analysis of the results reported in this study demonstrates that the same is true for the BCID calculations. Some solutions, such as solution B, can indeed be regarded as intruder solutions. In the quasidegenerate region, solution B gives excellent value of energy of state 3^1A_g (cf. Table I and Fig. 1) and unphysical wave functions. The proximity of the corresponding $\mathcal{M}^{\text{BCID}}$ and $\mathcal{M}_0^{(1)}$ spaces is significantly smaller, when compared with the value of d characterizing solution A for $\alpha \simeq 2.0a_0$. However, as α increases, the proximity d characterizing solution B increases and becomes larger than the value of d characterizing the physical solution A (cf. Table II). Solution B and the corresponding state 3^1A_g gain significant $\mathcal{M}_0^{(1)}$ components, so that one can accidentally converge to solution B with standard numerical procedures instead of obtaining solution A. One can equally accidentally converge to the other intruder solutions, such as C, D, E, F, and G in the region of large α values, which indicates that the intruder solution problem is a direct consequence of using the Bloch equation. The fact that we use the CI-like parametrization in the BCID calculations or the CC-like parametrization in the SUCCD calculations is of secondary importance here. The fact that the seriousness of the intruder state (or intruder solution) problem is almost identical in the BCID and SUCCD calculations can also be seen by comparing errors (relative to FCI) in the energies of the ground and the first-excited states obtained in both types of calculations at $\alpha = 6.0a_0$. These errors are 4.625 and 88.673 mhartree, respectively, for the BCID theory (cf. Tables II and VI), and 4.756 and 70.505 mhartree, respectively, for the SUCCD theory [14].

The incomplete model spaces, $\mathcal{M}_0^{(2)}$ and $\mathcal{M}_0^{(3)}$, provide us with examples of reference spaces that cannot simultaneously describe all M ($M = 3$, in the $\mathcal{M}_0^{(2)}$ case, and $M = 7$, in the $\mathcal{M}_0^{(3)}$ case) eigenstates $|\Psi_{\mu}\rangle$. For example, the three-dimensional

model space $\mathcal{M}_0^{(2)}$ can provide a reasonable zero-order approximation for only two lowest FCI states in the $\alpha \simeq 2.0a_0$ region. None of the remaining six FCI states can be accurately described by $\mathcal{M}_0^{(2)}$ (see the values of $S_{p_2}^{(\mu)}$ in Table VI). The $|\Psi_4^{\text{FCI}}\rangle$ and $|\Psi_6^{\text{FCI}}\rangle$ states have relatively large $\mathcal{M}_0^{(2)}$ components ($S_{p_2}^{(4)} = 0.45264$ and $S_{p_2}^{(6)} = 0.38298$), but they are not nearly as large as in the case of $|\Psi_1^{\text{FCI}}\rangle$ and $|\Psi_2^{\text{FCI}}\rangle$ ($S_{p_2}^{(1)} = 0.94977$ and $S_{p_2}^{(2)} = 0.94153$; cf. Table VI). For $\alpha = 6.0a_0$, the situation is even worse, since the only state that is dominated by configurations from $\mathcal{M}_0^{(2)}$ is the ground state.

An interesting situation is observed in the case of the seven-dimensional model space $\mathcal{M}_0^{(3)}$. In this case, all but one configurations are in the reference space and yet six, rather than seven, states $|\Psi_\mu^{\text{FCI}}\rangle$, $\mu = 1-6$, can accurately be described by the $\mathcal{M}_0^{(3)}$ configurations in the $\alpha \simeq 2.0a_0$ region (see the values of $S_{p_3}^{(\mu)}$ in Table VI). Only when α is large (e.g., $\alpha = 6.0a_0$), the $\mathcal{M}_0^{(3)}$ space provides an accurate zero-order approximation of $M = 7$ states $|\Psi_\mu^{\text{FCI}}\rangle$ ($|\Psi_\mu^{\text{FCI}}\rangle$, $\mu = 1-6, 8$). The $|\Psi_8^{\text{FCI}}\rangle$ state, which has a small $\mathcal{M}_0^{(3)}$ component in the $\alpha \simeq 2.0a_0$ region, gains a significant $\mathcal{M}_0^{(3)}$ component when α approaches large values (see the values of $S_{p_3}^{(\mu)}$ in Table VI). The $|\Psi_7^{\text{FCI}}\rangle$ state cannot be described by $\mathcal{M}_0^{(3)}$ for large α values, since it is virtually orthogonal to $\mathcal{M}_0^{(3)}$ in this region.

The magnitude of the $\mathcal{M}_0^{(2)}$ and $\mathcal{M}_0^{(3)}$ contributions to FCI states $|\Psi_\mu^{\text{FCI}}\rangle$ determines the quality of the BCID solutions. Let us begin our discussion with the BCID results obtained for the three-dimensional model space $\mathcal{M}_0^{(2)}$. In the region of small α values, there are only two solutions that are characterized by the proximities $d > 2.0$, namely, the physical solution labeled in Tables III and IV by I and the solution labeled in Tables III and IV by II. For $\alpha = 2.1a_0$, the value of d for solution I is 2.445, which should be compared to the upper bound for d in this case, i.e., $d = 3.0$. Large value of d characterizing solution I results in relatively reasonable description of these three states that have large $\mathcal{M}_0^{(2)}$ components, i.e., 1^1A_g , 2^1A_g , and 6^1A_g (at $\alpha = 2.1a_0$, the errors in the calculated energies, relative to FCI, are 1.304, 5.813, and 39.262 mhartree, respectively; cf. Tables III and VI). The 39.262 mhartree error obtained at $\alpha = 2.1a_0$ for state 6^1A_g is a consequence of a rather small $\mathcal{M}_0^{(2)}$ contribution to $|\Psi_6^{\text{FCI}}\rangle$ ($S_{p_2}^{(6)} = 0.38298$ at $\alpha = 2.1a_0$; cf. Table VI). Although description of the ground state by solution I is better

than the description of this state by solution A of Tables I and II, the description of the first-excited state, which has a large $\mathcal{M}_0^{(2)}$ component, by solution I is not particularly impressive (error of 5.813 mhartree at $\alpha = 2.1a_0$). This implies that the intruder state or intruder solution problem is more serious when the two-dimensional model space $\mathcal{M}_0^{(1)}$ is replaced by the three-dimensional model space $\mathcal{M}_0^{(2)}$. This can be understood if we realize that there is one more solution (solution II) that is characterized by the proximity $d > 2.0$ in the $\alpha \simeq 2.0a_0$ region and that there are many (17) real solutions with real energies that are characterized by $d > 1.0$. Solution II provides an excellent description of the ground state and a relatively reasonable description of the first-excited state (at $\alpha = 2.1a_0$, the errors relative to the FCI values of ΔE_1 and ΔE_2 are 2.023 and 9.808 mhartree, respectively; cf. Tables III and VI). Some solutions that are characterized by $d > 1.0$ in the $\alpha \simeq 2.0a_0$ region provide excellent description of the ground state (cf. solution 19 in Table III) or the first-excited state (cf. solutions 38 and 39 in Table III). As in the case of $\mathcal{M}_0^{(1)}$, and as can be seen in Table III, there are also many solutions that provide excellent values of energies of states that for $\alpha \simeq 2.0a_0$ are almost orthogonal to $\mathcal{M}_0^{(2)}$ (5^1A_g , 7^1A_g , 8^1A_g) or that are dominated by the \mathcal{M}_C configurations (5^1A_g ; see the values of $S_{p_2}^{(\mu)}$ and $S_{Q_{C3}}^{(\mu)}$ in Table VI). Solution III is in this category, since it provides excellent values of the energy of state 5^1A_g for $\alpha \simeq 2.0a_0$ (see the value of ΔE_3^{BCID} corresponding to solution III in Table III). In the $\alpha \simeq 2.0a_0$ region, solution III provides completely unphysical wave functions. However, as α becomes large, the ground-state and the first-excited-state wave functions and the corresponding energies obtained with solution III become quite realistic and some information is provided about state 6^1A_g . At $\alpha = 6.0a_0$, solution III provides description of the 1^1A_g , 2^1A_g , and 6^1A_g states that can compete with the description of these states provided by the physical solution I. The value of d characterizing solution III at $\alpha = 6.0a_0$ is comparable to the value of d characterizing solution I, which implies that solution III is an example of intruder solution. Other examples of intruder solutions are the above-mentioned solutions II and IV. Solution II provides a reasonable description of the lowest two states for all values of α , including large α values (e.g., $\alpha = 6.0a_0$; cf. Table IV). The corresponding value of the proximity d remains greater than 2.0 over the entire range of α values. In fact, when $\alpha = 6.0a_0$, the value of d characterizing solution II

is significantly larger than the value of d characterizing the physical solution I, although the errors in the BCID energies of the ground and the first-excited states obtained with solution II (2.955 and 59.630 mhartree, respectively) are larger than in the case of solution I (see Table IV). Solution IV provides better description of the ground and the first-excited states for larger α values than the physical solution I. Indeed, errors in the BCID energies of the ground and the first-excited states obtained with solution IV at $\alpha = 6.0a_0$ are only 0.192 and 4.267 mhartree, respectively (similar errors for solution I are 0.770 and 4.576 mhartree). Solution IV is not listed in Table III, since in the region of small α values it becomes complex. Thus, solution IV does not affect the BCID calculations of the ground and the first-excited states in the region of small α values, but for larger α values it changes its character so much that it provides better results for the lowest two states than the physical solution I.

Solutions II, III, and IV are examples of many solutions that may significantly affect our ability of converging the physical solution I with standard numerical procedures in the region of larger α values. For example, solutions I and III describe the same three states at $\alpha = 6.0a_0$ (1^1A_g , 2^1A_g , and 6^1A_g), so that it may not be obvious any more how to separate these two solutions in the BCID calculations employing standard numerical procedures. The fact that there are two solutions (I and II) in, what we normally call, the quasidegenerate region of the P4 model ($\alpha \simeq 2.0a_0$) shows that difficulties in converging solutions of genuine multireference theories that are based on the Bloch equation may be encountered in both degenerate and nondegenerate regions, particularly if the reference space is chosen poorly. Part of the problem may be the poorly defined model space and part of the problem is the Bloch formalism itself. The intruder state and intruder solution problems seem to be more severe when we increase the dimension of the model space. Similar remarks to this effect were made in Ref. [9], where the severity of the intruder state problem was analyzed in the context of SUCC calculations. It becomes clear now that the primary reason for the aggravation of the intruder state problem with M in genuine MRCC calculations is the steep increase in the number of solutions of the approximate Bloch equation with the dimension of \mathcal{M}_0 . Already for the simple minimum basis set P4 model, for which the dimension of the relevant FCI problem is only 8, there are as many as 336 solutions of the BCID equations, including 79 real solutions that give real

energies at $\alpha = 6.0a_0$. This should be compared to 56 solutions of the exact ($N_C = 8$, $M = 3$) BFCI theory and 50 solutions of the BCID equations for the two-dimensional model space $\mathcal{M}_0^{(1)}$.

Clearly, when the reference space becomes as large as $M = 7$ (the $\mathcal{M}_0^{(3)}$ case), in a situation where the dimension of the FCI problem, N_C , is only 8, the intruder solution problem should no longer be a major problem (which, of course, does not help much in practical applications of the Bloch formalism, since multireference calculations with spaces of the dimension comparable to that of the FCI problem are practically impossible and make no sense whatsoever). As already mentioned, the BCID equations employing $\mathcal{M}_0^{(3)}$ have only 7 solutions. On the other hand, it is interesting to analyze the $M = 7$ ($\mathcal{M}_0^{(3)}$) case, since even in this case, the use of the Bloch formalism leads to some unexpected problems.

In the region of large α values, the model space $\mathcal{M}_0^{(3)}$ provides excellent zero-order approximation of the target space spanned by FCI states μ^1A_g with $\mu = 1-6, 8$. The FCI expansions of these states are dominated by the $\mathcal{M}_0^{(3)}$ configurations in this region (see the values of $S_{p_3}^{(\mu)}$ in Table VI). The solution of the BCID equations that describes states μ^1A_g , $\mu = 1-6, 8$, is designated in Table V as solution 2. We refer to this solution as to the physical solution. For larger α values, solution 2 provides excellent description of the energies and wave functions of the FCI states μ^1A_g , $\mu = 1-6, 8$. At $\alpha = 6.0a_0$, the errors in the corresponding energies, relative to FCI, are 1.646, 0.000, 3.216, 0.046, 0.006, 0.042, and 0.000 mhartree, respectively (cf. Tables V and VI). The value of the proximity d characterizing this solution at $\alpha = 6.0a_0$, i.e., 6.866, is very close to the maximum value that d can assume in this case (7.0).

There are other solutions in this region that are characterized by large d values (solutions 1, 3, and 4), but these solutions provide unphysical wave functions, in spite of giving reasonably good energies of selected μ^1A_g states. For example, solution 1 provides reasonable values of energies of the first seven 1A_g states, although state 7^1A_g is virtually orthogonal to $\mathcal{M}_0^{(3)}$ for large α values and cannot be described by the BCID theory employing $\mathcal{M}_0^{(3)}$. Solution 3 provides reasonable estimates of energies of the FCI states $|\Psi_\mu^{\text{FCI}}\rangle$, $\mu = 1-4, 6-8$, including the energy of state 7^1A_g (at $\alpha = 6.0a_0$, the error relative to FCI, calculated by forming a difference of ΔE_6^{BCID} and ΔE_7^{FCI} is only 8.061 mhartree). Thus, solutions 1,

3, and 4 are examples of solutions resulting from the first part of our theorem. They provide excellent values of the energy of a state, which is virtually orthogonal to $\mathcal{M}_0^{(3)}$ and which cannot be described by the BCID theory.

In spite of the large values of d that characterize solutions 1, 3, and 4, these solutions cannot cause significant problems with obtaining the desired physical solution 2 of the BCID equations in the $\alpha \simeq 6.0a_0$ region, using standard numerical procedures, since the iterative BCID calculations would normally start from guessing the initial form of U by diagonalizing the Hamiltonian in $\mathcal{M}_0^{(3)}$. This can only give us good zero-order approximations for states $\mu^1 A_g$, $\mu = 1-6, 8$, that have large $\mathcal{M}_0^{(3)}$ components. By iterating the BCID equations, using the initial guess for U obtained by diagonalizing H in $\mathcal{M}_0^{(3)}$, we should easily obtain the physical solution 2. We can expect, however, significant problems with obtaining solution 2 in the $\alpha \simeq 2.0a_0$ region. In this region, diagonalization of H in $\mathcal{M}_0^{(3)}$ gives the wave functions that describe the $\mu^1 A_g$ states with $\mu = 1-7$, since these states are characterized by the largest $\mathcal{M}_0^{(3)}$ contributions in the $\alpha \simeq 2.0a_0$ region (see the values of $S_{P_3}^{(\mu)}$ in Table VI). In consequence, it is very likely that standard numerical procedures for solving nonlinear equations, when employed to BCID equations, will converge to solution 1 instead of 2.

It should be noticed that it is precisely solution 1 that in the $\alpha \simeq 6.0a_0$ region provides unphysical wave functions, while describing the energy of state $7^1 A_g$, which is virtually orthogonal to $\mathcal{M}_0^{(3)}$, that may cause problems with converging the physical solution 2. Thus, solution 1 is an example of the intruder solution discussed earlier in the context of solving the BCID equations with model spaces $\mathcal{M}_0^{(1)}$ and $\mathcal{M}_0^{(2)}$ and described in Ref. [14] in the context of solving the SUCCD equations. Solutions 3 and 4 are other examples of intruder solutions in the region of small α values. Solutions 1, 3, and 4 are characterized by large values of d in the $\alpha \simeq 2.0a_0$ region, so that they can be easier to converge with standard numerical procedures than the physical solution. Although the quality of the BCID results (particularly energies) obtained with solution 1 is equally good in the $\alpha \simeq 2.0a_0$ and large α regions, the intruder solution and intruder state problems do not seem to completely disappear when the dimension of the reference space is almost as large as the dimension of the FCI problem. Another interesting observation is that even when M is almost identical

to N_C , there still exist solutions of the BCID equations, such as solution 5 for $\alpha = 2.1a_0$, that give complex energies. This again shows that the nonlinear nature of the Bloch equation, combined with the asymmetric treatment of the $\mathcal{M}_0^{\perp(q)}$ subspaces in the BCID theory (the $\mathcal{M}_0^{\perp(q)}$ subspaces for different q values are not identical even when we use $\mathcal{M}_0^{(3)}$ as the model space), results in the appearance of pathological solutions of the truncated Bloch equations.

6. Formalism of β -Nested Equations in the Multireference Case

The interpretation of multiple solutions of the Bloch equation and the nature of the intruder solution problem plaguing the BCID approach can also be analyzed by establishing the relationships between solutions of the BCID and BFCI equations. In order to establish the relationships between multiple solutions corresponding to different approximations of the wave operator, it is useful to extend the single-reference formalism of β -nested equations (β -NEs) [24, 34] to the multireference case.

Let us consider two wave operators, both defined with respect to the same model space \mathcal{M}_0 , one defined as

$$U_A = \sum_{q=1}^M (1 + C_A^{(q)}) P_q, \quad (43)$$

where

$$C_A^{(q)} = \sum_{i=1}^{m_A} C_i^{(q)}, \quad (q = 1, \dots, M), \quad (44)$$

describing the approximate Bloch formalism referred to as method A, and another one, in which the wave operator U has the form

$$U_B = \sum_{q=1}^M (1 + C_B^{(q)}) P_q, \quad (45)$$

where

$$C_B^{(q)} = \sum_{i=1}^{m_B} C_i^{(q)}, \quad (m_B > m_A; q = 1, \dots, M), \quad (46)$$

describing the approximate ($m_B < N$) or exact ($m_B = N$) Bloch formalism, referred to as method B. Since $m_B > m_A$, method B can be viewed as an extension of method A.

The equations for the wave operator U_A and for the corresponding effective Hamiltonian $H_A^{\text{eff}}(U_A)$

can be given the following form [cf. Eqs. (10) and (41)]:

$$Q_A^{(p)} H U_A |\Phi_p\rangle = Q_A^{(p)} U_A P H_A^{\text{eff}}(U_A) |\Phi_p\rangle, \quad (p = 1, \dots, M), \quad (47)$$

$$H_A^{\text{eff}}(U_A) = P H U_A P, \quad (48)$$

$$Q_A^{(p)} = \sum_{i=1}^{m_A} Q_i^{(p)}, \quad (p = 1, \dots, M), \quad (49)$$

where $Q_i^{(p)} = \sum_{I^{(i)}} \langle \Phi_p | G_{I^{(i)}}^{(p)} | \Phi_p \rangle G_{I^{(i)}}^{(p)\dagger}$ is a projection operator onto the i -fold excited configurations relative to $|\Phi_p\rangle$ belonging to \mathcal{M}_0^\perp . In a similar way, we can obtain the equations defining method B,

$$Q_B^{(p)} H U_B |\Phi_p\rangle = Q_B^{(p)} U_B P H_B^{\text{eff}}(U_B) |\Phi_p\rangle, \quad (p = 1, \dots, M), \quad (50)$$

$$H_B^{\text{eff}}(U_B) = P H U_B P, \quad (51)$$

$$Q_B^{(p)} = \sum_{i=1}^{m_B} Q_i^{(p)}, \quad (p = 1, \dots, M). \quad (52)$$

Let us decompose the wave operator U_B and the projection operators $Q_B^{(q)}$, $q = 1, \dots, M$, as follows:

$$U_B = U_A + X_R, \quad (53)$$

$$Q_B^{(q)} = Q_A^{(q)} + Q_R^{(q)}, \quad (q = 1, \dots, M), \quad (54)$$

where

$$X_R = \sum_{q=1}^M \sum_{i=m_A+1}^{m_B} C_i^{(q)} P_q, \quad (55)$$

and

$$Q_R^{(q)} = \sum_{i=m_A+1}^{m_B} Q_i^{(q)}, \quad (q = 1, \dots, M). \quad (56)$$

Based on the above decompositions, the equations defining method B can be replaced by a system of equations:

$$\begin{aligned} Q_A^{(p)} H(U_A + X_R) |\Phi_p\rangle &= Q_A^{(p)} (U_A + X_R) P H_B^{\text{eff}}(U_A + X_R) |\Phi_p\rangle, \\ &(p = 1, \dots, M), \end{aligned} \quad (57)$$

$$\begin{aligned} Q_R^{(p)} H(U_A + X_R) |\Phi_p\rangle &= Q_R^{(p)} (U_A + X_R) P H_B^{\text{eff}}(U_A + X_R) |\Phi_p\rangle, \\ &(p = 1, \dots, M), \end{aligned} \quad (58)$$

$$H_B^{\text{eff}}(U_A + X_R) = P H(U_A + X_R) P. \quad (59)$$

In complete analogy with the β -NE formalism for a single-reference case [24, 34], we introduce the con-

tinuation parameter β in the following way:

$$\begin{aligned} Q_A^{(p)} H[U_A(\beta) + \beta X_R(\beta)] |\Phi_p\rangle &= Q_A^{(p)} [U_A(\beta) + \beta X_R(\beta)] P H^{\text{eff}}(\beta) |\Phi_p\rangle, \\ &(p = 1, \dots, M), \end{aligned} \quad (60)$$

$$\begin{aligned} \beta Q_R^{(p)} H[U_A(\beta) + X_R(\beta)] |\Phi_p\rangle &= \beta Q_R^{(p)} [U_A(\beta) + X_R(\beta)] P H^{\text{eff}}(\beta) |\Phi_p\rangle, \\ &(p = 1, \dots, M), \end{aligned} \quad (61)$$

$$H^{\text{eff}}(\beta) = P H[U_A(\beta) + \beta X_R(\beta)] P. \quad (62)$$

Equations (60)–(62) form a system of bilinear equations for the unknown matrix elements defining the operators $U_A(\beta)$, $X_R(\beta)$, and $H^{\text{eff}}(\beta)$. For $\beta = 0$, Eqs. (60)–(62) reduce to Eqs. (47) and (48), defining method A, provided that we identify $U_A(0)$ with U_A and $H^{\text{eff}}(0)$ with H_A^{eff} . For $\beta = 1$, Eqs. (60)–(62) reduce to Eqs. (50) and (51) or (57)–(59), defining method B, provided that we identify $U_A(1) + X_R(1)$ with U_B and $H^{\text{eff}}(1)$ with H_B^{eff} . Each solution

$$(U_A(\beta), X_R(\beta), H^{\text{eff}}(\beta)) \quad (63)$$

of the multireference β -nested equations [(60)–(62)] is a function of the parameter $\beta \in [0, 1]$, which for $\beta = 0$ gives a solution of equations representing method A [$U_A(0) = U_A$, $H^{\text{eff}}(0) = H_A^{\text{eff}}$] and which for $\beta = 1$ gives a solution of equations representing method B [$U_A(1) + X_R(1) = U_B$, $H^{\text{eff}}(1) = H_B^{\text{eff}}$]. We should notice that the operator

$$X_R(0) \equiv \lim_{\beta \rightarrow 0^+} X_R(\beta) \quad (64)$$

does not vanish. Once the $U_A \equiv U_A(0)$ and $H_A^{\text{eff}} \equiv H^{\text{eff}}(0)$ operators are determined by solving Eqs. (47) and (48), defining method A, we determine the operator $X_R(0)$ by solving the equations [cf. Eq. (61)],

$$\begin{aligned} Q_R^{(p)} H[U_A + X_R(0)] |\Phi_p\rangle &= Q_R^{(p)} [U_A + X_R(0)] \\ &\times P H_A^{\text{eff}} |\Phi_p\rangle, \quad (p = 1, \dots, M). \end{aligned} \quad (65)$$

The multireference procedure of β -nested equations works as follows: We first solve Eqs. (47), (48), and (65), defining method A, to obtain all solutions of Eqs. (60)–(62) in the $\beta = 0$ limit. Next, we solve Eqs. (50) and (51), defining method B, to obtain all solutions of Eqs. (60)–(62) in the $\beta = 1$ limit. Each $\beta = 0$ solution of Eqs. (60)–(62), i.e., $(U_A(0), X_R(0), H^{\text{eff}}(0))$, is continued toward the $\beta = 1$ limit and vice versa, each $\beta = 1$ solution of Eqs. (60)–(62), i.e., $(U_A(1), X_R(1), H^{\text{eff}}(1))$, is continued toward the $\beta = 0$ limit. Both continuations can easily be carried out using the Newton–Raphson

procedure, in which the solution $(U_A(\beta_0 + \Delta\beta), X_R(\beta_0 + \Delta\beta), H^{\text{eff}}(\beta_0 + \Delta\beta))$ is obtained by continuing the solution $(U_A(\beta_0), X_R(\beta_0), H^{\text{eff}}(\beta_0))$ determined earlier by solving Eqs. (60)–(62) at $\beta = \beta_0$. In order to make sure that the continuations of solutions from the $\beta = 0$ limit to the $\beta = 1$ limit and from the $\beta = 1$ limit to the $\beta = 0$ limit are carried out correctly, we used steps $\Delta\beta$ as small as ± 0.001 .

The above procedure of multireference β -nested equations was implemented and applied to establish the relationships between multiple solutions of the BCID (method A) and BFCI (method B) equations for the minimum basis set P4 model. The two-dimensional model space $\mathcal{M}_0^{(1)}$ was employed. Let us recall that in this case, there are 50 solutions of the BCID equations and 28 solutions of the BFCI equations.

Two representative values of α were investigated, namely, $\alpha = 2.1a_0$ (the quasidegenerate region) and $\alpha = 6.0a_0$ (the nondegenerate region). For $\alpha = 2.1a_0$, there are 17 solutions of the BCID equations that can smoothly be continued to the $\beta = 1$ (BFCI) limit. The remaining 33 solutions of the BCID equations and the remaining 11 solutions of the BFCI equations cannot be continued between the $\beta = 0$ and $\beta = 1$ limits. The corresponding operator functions $(U_A(\beta), X_R(\beta), H^{\text{eff}}(\beta))$ have branch point singularities and/or poles along the real β axis. The fact that so few solutions of the BCID equations can smoothly be continued to the $\beta = 1$ limit clearly demonstrates that the large majority of the BCID solutions are completely unphysical. For $\alpha = 6.0a_0$, the number of solutions of the BCID equations that can smoothly be continued to the exact $\beta = 1$ limit is 13. Among them, there are several solutions of the BCID equations, such as solutions B and E discussed in Section 5, that provide better description of either the ground state (solution B) or the first-excited state (solution E) in the nondegenerate region than the description of these states provided by the physical solution A (cf. Tables I and II). Let us analyze the corresponding energy functions $\Delta E_\mu(\beta) = E_\mu(\beta) - \langle \Phi_1 | H | \Phi_1 \rangle$, $\mu = 1, 2$ (referred to as the β -NE energies), obtained by diagonalizing the β -dependent effective Hamiltonian $H^{\text{eff}}(\beta)$, Eq. (62), in the reference space $\mathcal{M}_0^{(1)}$, for $\alpha = 2.1a_0$ and $\alpha = 6.0a_0$. We focus on the energy functions $\Delta E_\mu(\beta)$, obtained by continuing solutions A, B, and E from $\beta = 0$ to $\beta = 1$, since solution A is a physical solution representing the ground and the first-excited state and solutions B and E are examples of intruder solutions causing problems with converging the physical solution in the nondegenerate region.

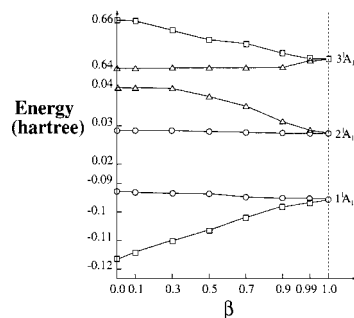


FIGURE 3. Relations between selected solutions of the BCID and BFCI equations for the P4 model system with $\alpha = 2.1a_0$ as represented by the corresponding β -NE energies $\Delta E_\mu(\beta) = E_\mu(\beta) - \langle \Phi_1 | H | \Phi_1 \rangle$, $\mu = 1, 2$ (in hartree), obtained by diagonalizing the β -dependent effective Hamiltonian $H^{\text{eff}}(\beta)$, Eq. (62), in the reference space $\mathcal{M}_0^{(1)}$. The β -NE energies $\Delta E_\mu(\beta)$, $\mu = 1, 2$, corresponding to solutions A, B, and E are marked by \circ , \square , and \triangle , respectively.

The dependencies of the β -NE energies, $\Delta E_\mu^X(\beta)$, $\mu = 1, 2$, $X = A, B, E$, obtained by continuing the BCID solutions A, B, and E from $\beta = 0$ to $\beta = 1$, are shown in Figures 3 ($\alpha = 2.1a_0$) and 4 ($\alpha = 6.0a_0$). The physical character of solution A manifests itself in the fact that the continuation of this solution along the real β axis gives the two lowest $1A_g$ FCI states (cf. Figs. 3 and 4). Solution B, when continued toward the $\beta = 1$ limit, gives the FCI states 1^1A_g and 3^1A_g , whereas the continuation of solution E toward the $\beta = 1$ limit gives the FCI states $|\Psi_2^{\text{FCI}}\rangle$ and

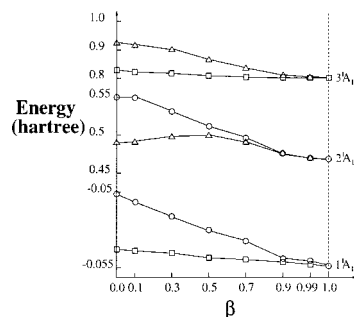


FIGURE 4. Relations between selected solutions of the BCID and BFCI equations for the P4 model system with $\alpha = 6.0a_0$ as represented by the corresponding β -NE energies $\Delta E_\mu(\beta) = E_\mu(\beta) - \langle \Phi_1 | H | \Phi_1 \rangle$, $\mu = 1, 2$ (in hartree), obtained by diagonalizing the β -dependent effective Hamiltonian $H^{\text{eff}}(\beta)$, Eq. (62), in the reference space $\mathcal{M}_0^{(1)}$. The β -NE energies $\Delta E_\mu(\beta)$, $\mu = 1, 2$, corresponding to solutions A, B, and E are marked by \circ , \square , and \triangle , respectively.

$|\Psi_3^{\text{FCI}}\rangle$). Thus, the formalism of β -nested equations provides us with a well-defined procedure of identifying solutions of the BCID equations with pairs (in general, M -tuples) of FCI states, into which the BCID states evolve as $\beta \rightarrow 0$. We could also try to identify the BCID solutions by finding these two FCI states, $|\Psi_{\kappa_1}^{\text{FCI}}\rangle$ and $|\Psi_{\kappa_2}^{\text{FCI}}\rangle$, that give the largest value of the proximity $\Delta_{\kappa_1\kappa_2}$ between the BCID and BFCI target spaces [see Eqs. (34) and (35)]. In the case of solution A, the maximum value of $\Delta_{\kappa_1\kappa_2}$ is obtained when $\kappa_1 = 1$ and $\kappa_2 = 2$, which shows that solution A approximates the pair of FCI states $|\Psi_1^{\text{FCI}}\rangle$ and $|\Psi_2^{\text{FCI}}\rangle$. There are, however, cases where the identification of solutions of the BCID equations based on the searching for the maximum value of $\Delta_{\kappa_1\kappa_2}$ leads to uncertain results. For example, the largest value of the proximity $\Delta_{\kappa_1\kappa_2}$ for solution E at $\alpha = 6.0a_0$ is obtained when $\kappa_1 = 2$ and $\kappa_2 = 4$ ($\Delta_{24} = 1.780$ in this case; the value of Δ_{23} for solution E at $\alpha = 6.0a_0$ is 1.675). The β -NE continuation procedure clearly shows that independent of the value of α , solution E evolves into the exact solution that describes the $|\Psi_2^{\text{FCI}}\rangle$ and $|\Psi_3^{\text{FCI}}\rangle$ states. The β -NE formalism provides us with a more rigorous way of identifying the solutions of the approximate Bloch equation. On the other hand, the identification method based on searching for the maximum value of $\Delta_{\kappa_1\dots\kappa_M}$ has an advantage that we can apply it even to solutions of the approximate Bloch equation that cannot be continued to the exact ($\beta = 1$) limit along the real β axis.

The β -NE formalism provides us with an interesting way of looking at the intruder solution problem. In the quasidegenerate region (e.g., for $\alpha = 2.1a_0$; see Fig. 3), the β -NE energies $\Delta E_\mu^A(\beta)$, $\mu = 1, 2$, corresponding to the physical solution A, are virtually independent of β . In this region, the values of $\Delta E_1^A(\beta)$ and $\Delta E_2^A(\beta)$ are practically identical to the exact energies of states 1^1A_g and 2^1A_g , ΔE_1^{FCI} and ΔE_2^{FCI} , respectively. At the same time, the β -NE energies $\Delta E_\mu^B(\beta)$ and $\Delta E_\mu^E(\beta)$, $\mu = 1, 2$, obtained by continuing solutions B and E toward $\beta = 1$, display a significant dependence on β . Except for the immediate vicinity of $\beta = 1$, the differences between the values of $\Delta E_\mu^B(\beta)$ and $\Delta E_\mu^E(\beta)$ and the energies of the corresponding FCI states, into which solution B and E evolve, are very large (see Fig. 3). The description of the energies of the lowest two 1^1A_g states provided by solution A is far better than the description of the energies of these states provided by solutions B and E.

The situation changes as α approaches large values. For $\alpha = 6.0a_0$, the energy functions $\Delta E_\mu^A(\beta)$, $\mu = 1, 2$, corresponding to solution A, strongly vary with

β (see Fig. 4). Except for the immediate vicinity of $\beta = 1$, the values of $\Delta E_\mu^A(\beta)$ significantly differ from the energies of the lowest two 1^1A_g states, into which $\Delta E_\mu^A(\beta)$ evolve as $\beta \rightarrow 1$. The values of function $\Delta E_1^B(\beta)$, including the $\beta = 0$ value or the BCID energy provided by solution B, are much closer to the exact ground-state energy ΔE_1^{FCI} than the values of function $\Delta E_1^A(\beta)$ obtained by continuing solution A. In fact, both energy functions $\Delta E_\mu^B(\beta)$, $\mu = 1, 2$, are practically independent of β , providing excellent agreement with the exact energies of states 1^1A_g and 3^1A_g (cf. Fig. 4). The description of states 1^1A_g and 3^1A_g by solution B is evidently much better than the description of the lowest two states by solution A in this region. This clearly shows the intruder nature of solution B. Similar remarks apply to solution E. The values of $\Delta E_1^E(\beta)$, including the BCID energy obtained at $\beta = 0$, are much closer to the exact energy of the first-excited state than the values of $\Delta E_2^A(\beta)$ obtained by continuing solution A. The energy function $\Delta E_1^E(\beta)$ displays a small dependence on β , but this dependence is much weaker than the dependence of $\Delta E_2^A(\beta)$ on β . This demonstrates the intruder nature of solution E at $\alpha = 6.0a_0$.

In general, we may expect that intruder solutions of the approximate Bloch equation are characterized by the strong variation of the corresponding β -NE energies $\Delta E_\mu(\beta)$ with β in the quasidegenerate region and a rather weak dependence of most or all of the energies $\Delta E_\mu(\beta)$ on β in regions where the intruder solution (or intruder state) problem becomes severe. The only solution that is expected to exhibit a weak dependence of energies $\Delta E_\mu(\beta)$ on β in the quasidegenerate region is the physical solution.

7. Summary and Concluding Remarks

In this study, we used the homotopy method to find complete sets of solutions of the Bloch equation for a four-electron system, referred to as the P4 model. We considered different forms of the Bloch equation corresponding to various choices of the model space and different approximations of the wave operator. We focused on simple, linear, CI-like parametrizations of the Bloch wave operator, so that we could investigate to what extent problems plaguing genuine multireference methods, such as the intruder solution problem plaguing the SUCC method, are a consequence of using the Bloch equation.

We demonstrated that the number of solutions of the Bloch equation employing an approximate form

of the wave operator may significantly exceed the number of solutions of the exact Bloch equation, even when the approximate form of the wave operator is extremely simple, so that the nonlinearity of the problem remains low. We also demonstrated that the number of solutions of the exact Bloch equation equals $\binom{N_C}{M}$, where N_C is the dimension of the relevant FCI subproblem and M is the dimension of the model space. We emphasized the fact that the most natural truncation schemes for the excitation operators entering the Bloch equation result in the asymmetric treatment of manifolds of excitations corresponding to different reference configurations. From the practical point of view, one should view all these characteristics of the Bloch equation formalism as serious drawbacks, since even for model spaces of small or medium size the total number of solutions of the Bloch equation may be overwhelmingly large and many solutions of the approximate schemes based on the Bloch equation may be completely pathological. As demonstrated earlier [14], the large number of solutions of the Bloch equation increases even further when the nonlinear CC parametrization is employed to construct the wave operator.

The intruder solution problem plaguing the SUCC theory [14] was shown to be almost equally serious when the nonlinear parametrization of the wave operator used in the SUCC theory was replaced by the simple CI-like (i.e., linear) parametrizations. As in the SUCC calculations, there exists a class of solutions of the approximate Bloch equations that are characterized by small overlaps with the reference space in the quasidegenerate region and large overlaps with the model space in other regions of nuclear geometries. In the quasidegenerate region, these solutions provide almost exact energies of one or more states that are virtually orthogonal to the model space, although the corresponding wave functions are completely unphysical. These solutions may cause problems with converging the desired physical solution of the Bloch equation in the nondegenerate region, once the resulting wave functions gain significant reference-space components. For this reason, we call these solutions the intruder solutions. The study reported in this work shows that the intruder solution problem plaguing genuine multireference calculations is primarily caused by the bilinearity of the Bloch equation, and, to some extent, by the asymmetric treatment of the excitation manifolds corresponding to different references in approximate methods, much less by the particular form of the wave operator (CI-like, CC-

like, etc.) used in the calculations. We also demonstrated that for $M \ll N_C$, the severity of the intruder solution problem in calculations based on the Bloch wave operator formalism increases with the dimension of the model space. The number of intruder solutions may significantly increase with M , particularly when the model space \mathcal{M}_0 is chosen poorly. Surprising enough, even when the dimension of the model space is very large, so that $M \simeq N_C$, there may exist a few solutions of the approximate Bloch equation that can cause problems with obtaining the desired physical solution, when standard numerical procedures are employed.

The nature of intruder solutions was also analyzed by continuing the solutions of the approximate Bloch equation to the exact limit by solving the so-called β -nested equations (β is the appropriate continuation parameter). It was demonstrated that in the quasidegenerate region the β -dependent energies obtained by continuing intruder solutions toward the exact limit strongly vary with β . Similar energies characterizing the physical solution of truncated Bloch equation are virtually independent of β in the same region. In the nondegenerate region, the β -dependent energies obtained by continuing the physical solution toward the exact limit strongly vary with β . At least some energies characterizing intruder solutions display a much weaker β dependence, providing a much better description of the FCI states than that provided by the physical solution.

Even when the wave operator is parametrized in a simple way, such as that used in the BCID approach, the approximate Bloch equation may have both real and complex solutions. Some real solutions lead to effective Hamiltonians that have complex eigenvalues. Similar behavior was observed in Refs. [9, 10], where it was shown that the linearized form of truncated SUCC equations may have real solutions that lead to complex eigenvalues of H^{eff} .

The present study suggests that in further development of genuine MRCC theories that are based on the Bloch formalism, one should focus on modifying the existing equations, so that the desired physical solution is clearly isolated from other solutions of the corresponding nonlinear equations. One such method was briefly discussed in Ref. [14]. Another interesting implication of the approach discussed in this work is the idea of solving the matrix form of the Bloch equation directly, i.e., without assuming a particular form of the wave operator in the process of evaluating U . In the existing MRCC approaches of the SUCC or VUCC type, the CC para-

metrization of the wave operator is introduced into the Bloch equation and the resulting highly nonlinear equations for cluster amplitudes are derived and programmed. This approach leads to various mathematical problems, such as problems with the generalization of the SUCC theory to arbitrary reference spaces and states of arbitrary multiplicity (the current state-of-the-art orthogonally spin-adapted SUCCSD method is designed to handle only two totally symmetric singlet states described by the model space spanned by two closed-shell configurations [11]). A much simpler idea might be to solve the matrix Bloch equation for the matrix elements U_{kp} [cf. Eqs. (22) and (23)] directly, by using one of the available iterative algorithms for solving the CI-type equations, while introducing the CC (e.g., SUCC) parametrization for U in every iteration of the iterative procedure by simply relating matrix elements U_{kp} to pertinent cluster amplitudes. An approach of this type would eliminate the need for deriving first the complicated orthogonally spin-adapted MRCC (e.g., SUCC) equations. The orthogonal spin adaptation of the matrix Bloch equation and the extensions of the Bloch equation to arbitrary model spaces seem relatively straightforward. Enforcing the CC parametrization for U in every iteration of the algorithm used to solve the matrix Bloch equation would be fully equivalent to the process of solving the nonlinear MRCC equations, without deriving the explicit MRCC equations. It would also allow us to implement new variants of the MRCC theory, in which manifolds of excitations used to define cluster operators $T^{(p)}$ for different references $|\Phi_p\rangle$ are identical. Ideas of this type are currently explored in our group.

ACKNOWLEDGMENTS

One of us (P.P.) would like to thank John Wiley & Sons, Inc. and the organizers of the 40th Sanibel Symposium for presenting to him the First Wiley-International Journal of Quantum Chemistry Young Investigator Award. The Quantum Theory Project Fellowship to attend the 40th Sanibel Symposium awarded to K.K. is greatly appreciated, too. Both awards allowed the authors to present the results described in this work at the 40th Sanibel Symposium. We are very much indebted to the reviewer for a very insightful analysis of our results and for helpful remarks that allowed us to considerably improve our discussion. This work has been supported by the startup funds provided to one of us (P.P.) by Michigan State University.

References

- Bloch, C. Nucl Phys 1958, 6, 329.
- Jørgensen, F. Mol Phys 1975, 29, 1137.
- Durand, Ph. Phys Rev A 1983, 28, 3184.
- Jeziorski, B.; Monkhorst, H. J. Phys Rev A 1981, 24, 1668.
- Jeziorski, B.; Paldus, J. J Chem Phys 1988, 88, 5673.
- Paldus, J.; Pylypow, L.; Jeziorski, B. in Many-Body Methods in Quantum Chemistry; Kaldor, U., Ed.; Lecture Notes in Chemistry, Vol. 52; Springer: Berlin, 1989; pp. 151–170.
- Piecuch, P.; Paldus, J. Theor Chim Acta 1992, 83, 69.
- Paldus, J.; Piecuch, P.; Jeziorski, B.; Pylypow, L. in Recent Progress in Many-Body Theories; Ainsworth, T. L.; Campbell, C. E.; Clements, B. E.; Krotschek, E., Eds.; Plenum: New York, 1992; Vol. 3, pp. 287–303.
- Paldus, J.; Piecuch, P.; Pylypow, L.; Jeziorski, B. Phys Rev A 1993, 47, 2738.
- Piecuch, P.; Paldus, J. Phys Rev A 1993, 49, 3479.
- Piecuch, P.; Paldus, J. J Chem Phys 1994, 101, 5875.
- Piecuch, P.; Paldus, J. J Phys Chem 1995, 99, 15354.
- Piecuch, P.; Landman, J. I. Parallel Comp 2000, 26, 913.
- Kowalski, K.; Piecuch, P. Phys Rev A 2000, 61, 052506.
- Meissner, L.; Jankowski, K.; Wasilewski, J. Int J Quantum Chem 1988, 34, 535; Meissner, L.; Kucharski, S. A.; Bartlett, R. J. J Chem Phys 1989, 91, 6187; Meissner, L.; Bartlett, R. J. Ibid. 1990, 92, 561; Kucharski, S. A.; Bartlett, R. J. Ibid. 1991, 95, 8227; Balková, A.; Kucharski, S. A.; Meissner, L.; Bartlett, R. J. Theor Chim Acta 1991, 80, 335.
- Berkovic, S.; Kaldor, U. Chem Phys Lett 1992, 199, 42; J Chem Phys 1993, 98, 3090.
- Paldus, J. in Methods in Computational Molecular Physics; Wilson, S.; Diercks, G. H. F., Eds.; Plenum: New York, 1992; pp. 99–194; Paldus, J.; Li, X. Adv Chem Phys 1999, 110, 1.
- Lindgren, I.; Mukherjee, D. Phys Rep 1987, 151, 93; Mukherjee, D.; Pal, S. Adv Quantum Chem 1989, 20, 291; Bernholdt, D. E.; Bartlett, R. J. Adv Quantum Chem 1999, 34, 271.
- Jeziorski, B.; Paldus, J. J Chem Phys 1989, 90, 2714.
- Jankowski, K.; Paldus, J.; Grabowski, I.; Kowalski, K. J Chem Phys 1992, 97, 7600; 1994, 101, 1759 [Erratum]; Jankowski, K.; Paldus, J.; Grabowski, I.; Kowalski, K. Ibid. 1994, 101, 3085.
- Coester, F. Nucl Phys 1958, 7, 421; Coester, F.; Kümmel, H. Ibid. 1960, 17, 477; Čížek, J. J Chem Phys 1966, 45, 4256; Adv Chem Phys 1969, 14, 35; Čížek, J.; Paldus, J. Int J Quantum Chem 1971, 5, 359; Paldus, J.; Čížek, J.; Shavitt, I. Phys Rev A 1972, 5, 50.
- Bartlett, R. J. Ann Rev Phys Chem 1981, 32, 359; J Phys Chem 1989, 93, 1697; in Modern Electronic Structure Theory; Yarkony, D. R., Ed.; World Scientific: Singapore, 1995; Part I, pp. 1047–1131.
- Paldus, J. in New Horizons of Quantum Chemistry; Löwdin, P.-O.; Pullman, B., Eds.; Reidel: Dordrecht, 1983; pp. 31–60; Bartlett, R. J.; Dykstra, C. E.; Paldus, J. in Advanced Theories

- and Computational Approaches to the Electronic Structure of Molecules; Dykstra, C. E., Ed.; Reidel: Dordrecht, 1984; pp. 127–159.
24. Piecuch, P.; Kowalski, K. in *Computational Chemistry: Reviews of Current Trends*; Leszczyński, J., Ed.; World Scientific: Singapore, 2000; Vol. 5, pp. 1–105.
 25. Schucan, T. H.; Weidenmüller, H. A. *Ann Phys (NY)* 1972, 73, 108; *Ibid.* 1973, 76, 483.
 26. Hose, A.; Kaldor, U. *J Phys B* 1979, 12, 3827.
 27. Finley, J. P.; Chaudhuri, R. K.; Freed, K. F. *J Chem Phys* 1995, 103, 4990.
 28. Finley, J. P.; Freed, K. F. *J Chem Phys* 1995, 102, 1306; Finley, J. P.; Chaudhuri, R. K.; Freed, K. F. *Phys Rev A* 1996, 54, 343; Chaudhuri, R. K.; Freed, K. F. *J Chem Phys* 1997, 107, 6699.
 29. Zarrabian, S.; Paldus, J. *Int J Quantum Chem* 1990, 38, 761.
 30. Allgower, E. L.; Georg, K. *Numerical Continuation Methods*; Springer: Berlin, 1990; Morgan, A. P. *Solving Polynomial Systems Using Continuation for Scientific and Engineering Problems*; Prentice-Hall: Englewood Cliffs, NJ, 1987.
 31. Chow, S.-N.; Mallet-Paret, J.; Yorke, J. A. *Math Comput* 1978, 32, 887.
 32. Morgan, A. P.; Sommese, A. J.; Watson, L. T. *ACM Trans Math Software* 1989, 15, 93.
 33. Jankowski, K.; Paldus, J. *Int J Quantum Chem* 1980, 17, 1243.
 34. Jankowski, K.; Kowalski, K. *J Chem Phys* 1999, 111, 2952; Jankowski, K.; Kowalski, K.; Grabowski, I.; Monkhorst, H. *Int J Quantum Chem* 1999, 75, 483.
 35. Meißner, H.; Paldus, J. *J Chem Phys* 2000, 113, 2594; *Ibid.* 2000, 113, 2612; *Ibid.* 2000, 113, 2622.
 36. Meißner, H.; Steinborn, O. *Phys Rev A* 1997, 56, 1189; *Int J Quantum Chem* 1997, 61, 777; *Ibid.* 1997, 63, 257.
 37. Jankowski, K. *Int J Quantum Chem* 1976, 10, 683.
 38. Piecuch, P.; Oliphant, N.; Adamowicz, L. *J Chem Phys* 1993, 99, 1875; Piecuch, P.; Adamowicz, L. *J Chem Phys* 1994, 100, 5792.